Patterned Neuronal Activities Dictate Cell Type-specific Axon Regeneration

Kendra Takle Ruppell,[1,4] Fei Wang,[1,4] Feng Li,[2,4] Ye Shang,[1] Jiaxin Gong,[5] Pavi Guttipatti,[2] Yuanquan Song,[2,3] and Yang Xiang[1, 6, *]

[1]Department of Neurobiology, Program of Neuroscience, University of Massachusetts Medical School, 364 Plantation Street, Worcester, MA 01605, USA

[2]Raymond G. Perelman Center for Cellular and Molecular Therapeutics, The Children's Hospital of Philadelphia, Philadelphia, PA 19104, USA

[3]Department of Pathology and Laboratory Medicine, University of Pennsylvania, Philadelphia, PA 19104, USA

[4]These authors contributed equally

[5]Department of Neurobiology, University of Massachusetts Medical School, 364 Plantation Street, Worcester, MA 01605, USA

[6]Lead Contact

*Correspondence: yang.xiang@umassmed.edu (Y.X.)

Abstract

Injured neurons exhibit cell type-specific axon regeneration, but the underlying mechanisms remain elusive. Two subtypes of *Drosophila* sensory neurons show distinct regenerative competence. Here, we show that axotomy induces long-lasting burst firing and Ca^{2+} spikes specifically in the regenerative subtype. Genetic silencing of firing in the regenerative subtype inhibits regeneration. Optogenetic stimulation of the non-regenerative subtype reveals that activity patterns critically determine regeneration; burst firing triggers Ca^{2+} spikes and suffices to induce regeneration, while tonic firing fails to induce Ca^{2+} spikes and regeneration. We further show the L-type Ca^{2+} channel, Dmca1D, regulates Ca^{2+} spikes and regeneration. Intriguingly, the regenerative neuronal subtype expresses higher levels of Dmca1D, and overexpression of Dmca1D in the non-regenerative subtype facilitates regeneration. Our studies indicate that injury induces cell type-specific neuronal activities, which act through Ca^{2+} spikes to govern regeneration, and suggest that precise control of neuronal activity patterns is an effective way to promote regeneration.

Introduction

Injured neurons have limited ability to regenerate their axons, hindering the functional recovery after lesions of the nervous system. Studies in *C. elegans*, *Drosophila* and mice have uncovered evolutionarily conserved roles of intrinsic factors, such as mammalian target of rapamycin (mTOR) and dual leucine kinase (DLK), in controlling the axon regenerative capacity (Hammarlund et al., 2009; Park et al., 2008; Shin et al., 2012; Xiong et al., 2010; Yan et al., 2009). Importantly, recent studies have found that not all neurons regenerate equally. For example, alpha subtypes of retinal ganglion cells (αRGCs) preferentially regenerate when mTOR signaling is stimulated, while other RGC types fail to regenerate (Duan et al., 2015). This cell type-specific regeneration has also been observed in *Drosophila* and *C. elegans* (Ghosh-Roy and Chisholm, 2010; Song et al., 2012). For example, class IV dendritic arborization (C4da) neurons of *Drosophila* larvae regenerate after axotomy, while class III dendritic arborization (C3da) neurons, which share the same microenvironment with C4da neurons, fail to regenerate (Song et al., 2012). Understanding why only certain neuronal types are amendable to regeneration is crucial for designing cell type-specific therapeutic strategies to promote functional recovery.

Neuronal activity has long been recognized to critically regulate axon pathfinding during development (Singh and Miller, 2005; Spitzer, 2006; Zhang and Poo, 2001). Stimulation of neuronal activity has also been shown to promote axon regeneration by enhancing neuronal responses to neurotrophic factors (Brushart et al., 2002; Goldberg et al., 2002). Recent studies have shown that increasing neuronal activity in injured neurons, by overexpression of G protein-coupled receptor melanopsin, or designer

receptors exclusively activated by designer drugs (DREADD)-based chemogenetics, or by visual stimulation to the injured RGCs, facilitates axon regeneration (Li et al., 2016; Lim et al., 2016). In addition, silencing presynaptic amacrine cells or pharmacologically blocking inhibitory neurotransmission can elevate growth factor responsiveness of postsynaptic RGCs and promote axon regeneration (Zhang et al., 2019). Despite the importance of exogenously applied neuronal stimulation in promoting axon regeneration, it remains largely unknown how nerve injury affects the intrinsic neuronal excitability, and whether the intrinsic excitability plays a role in cell type-specific axon regeneration.

Intracellular Ca^{2+} signaling plays a key role in axon regeneration (He and Jin. 2016). As key regulators of axon regeneration, DLK and its *Drosophila* homolog Wallenda (Wnd) are activated downstream of Ca^{2+} signals (Hao and Collins, 2017; Tedeschi and Bradke, 2013; Xiong et al., 2010; Yan et al., 2009). In cultured mouse dorsal root ganglion (DRG) neurons and *Aplysia* neurons, local Ca^{2+} elevation promotes the formation of growth cones after transection (Chierzi et al., 2005; Kamber et al., 2009). In *C. elegans*, transient axotomy-induced Ca^{2+} influx *via* the voltage-gated calcium channel EGL-19 promotes regeneration and growth cone formation of the PLM sensory neuron (Ghosh-Roy et al., 2010). Moreover, a genetic screen in *C. elegans* has identified a cluster of genes affecting Ca^{2+} signaling and homeostasis to be critical for axon regeneration (Chen et al., 2011).

In the current study, we set out to determine the cellular and molecular mechanisms underlying cell type-specific regeneration, using the *Drosophila* C4da and C3da sensory neurons as a model. This system has several unique advantages. Firstly,

studies on neuronal functions, dendritic morphology and gene expression profiles indicate that C4da and C3da neurons belong to two distinct cell types. For example, C4da neurons express noxious stimulus-detecting transient receptor potential A1 (TrpA1) and are polymodal nociceptors, while C3da neurons express the mechanotransduction channel no mechanoreceptor potential C (NompC) and are gentle touch receptors (Tracey et al., 2003; Xiang et al., 2010; Yan et al., 2013). Secondly, C4da and C3da neurons can be unambiguously labeled, and their neuronal activities can be measured and manipulated at the single-cell resolution. Thirdly, larval cuticle is transparent, allowing axotomy, regeneration analysis and optogenetic stimulation in live animals *in vivo*.

Results

Axotomy Triggers Neuronal Subtype-specific Burst Firing

Cell bodies of *Drosophila* larval C3da and C4da neurons are near each other, and dendrites of these two neuronal types extensively overlap (Figure 1A). Moreover, axons of C3da and C4da neurons are ensheathed by the same glial cells (Han et al., 2011). These anatomical features suggest that C3da and C4da neurons share a similar physical and biochemical environment. Here, we delivered two-photon laser pulse to lesion the axon of either C3da or C4da neurons *in vivo* (Figure S1A). Live imaging showed no detectable damage to the ensheathing glial membrane (Figure S1B), indicating that the injury was local. At 24 hours post axotomy (hpa), extensive axon regrowth has not started (Song et al., 2012). To quantify axon regeneration, we measured the proximal axon length at 24 and 48 hpa to calculate the absolute

regeneration length (Figure S1A), as well as the regeneration index that takes into consideration larval body growth (see Methods for details). We found that axotomized C4da neurons displayed robust axon regrowth (Figure 1B, D), while in contrast, axotomized C3da neurons showed little regeneration (Figure 1C, E), consistent with the previous reports (Song et al., 2012). These results indicate that C4da and C3da neurons exhibit cell type-specific regeneration capacity, and this specificity may be attributable to intrinsic differences between these two neuronal subtypes.

To determine how axotomy affects neuronal excitability, and explore whether neuronal activity plays a role in cell-type specific regeneration, we performed extracellular recordings to measure spontaneous action potentials from intact and axotomized sensory neurons (Xiang et al., 2010). We found that axotomized C4da neurons exhibited robust and continuous burst firing at 24 hpa (Figure 1F, G). In sharp contrast, burst firing was not detected in intact C4da neurons recorded in the same larvae (Figure 1F, H). Here we defined a burst firing event as a cluster of five or more consecutive action potentials with an inter-spike interval of 100 ms or less (Figure S1C). The frequency of burst firing events was significantly increased by axotomy in C4da neurons (average burst firing events per minute was 0.00041 in intact and 4.2 in axotomized C4da neurons, Figure 1G). We detected robust burst firing in ~95% (18 of 19) of axotomized C4da neurons, in contrast to ~6% (1 of 17) in intact C4da neurons (Figure S1D). Moreover, 34.96% of action potentials in axotomized C4da neurons were detected in the burst firing events, in contrast to 0.17% in intact C4da neurons (Figure S1E). In addition to the induction of burst firing, axotomy also increased the overall excitability of C4da neurons, as the average baseline firing frequency was increased

from 0.57 Hz in intact C4da neurons to 1.14 Hz in axotomized C4da neurons (Figure 1I).

Next, we recorded spontaneous action potentials of axotomized C3da neurons at 24 hpa. As a control, we also recorded intact C3da neurons in the same larvae. We found that the firing patterns of axotomized and intact C3da neurons were comparable, with almost no burst firing detected (0.052 bursts/min in intact and 0.060 bursts/min in axotomized C3da neurons, Figure 1H), and the overall firing frequency was unchanged (0.33 Hz in intact and 0.23 Hz in axotomized C3da neurons, Figure 1J).

Together, these electrophysiological studies indicate that nerve injury modulates neuronal activities in a cell type-specific fashion; it profoundly regulates spontaneous activities of C4da neurons by transforming their firing pattern into the burst mode and increases their excitability, but has little effect on spontaneous activities of C3da neurons. Notably, the cell type-specific burst firing correlates with axon regeneration capacity.

Axotomy Triggers Neuronal Subtype-specific Ca^{2+} Spikes

Ca^{2+} signals critically control axon regeneration (He and Jin, 2016). To determine how axotomy regulates Ca^{2+} responses, we performed Ca^{2+} imaging using the genetically encoded Ca^{2+} indicator, GCaMP6s. We first assessed Ca^{2+} signals in C4da neurons by expressing *UAS-GCaMP6s* with and without injury. Intriguingly, we observed marked and continuous Ca^{2+} spikes in axotomized C4da neurons at 24 hpa, while no Ca^{2+} spikes were detected in intact C4da neurons (Figure 2A-B, S2A-C and supplemental video S1-S2. See Methods for Ca^{2+} spikes quantification). Careful

analysis revealed that Ca^{2+} spikes were temporally synchronized across the cell body, axon and dendrites, reflecting a global Ca^{2+} increase across the entire axotomized C4da neurons (Figure 2B). Ca^{2+} spikes were completely abolished in the absence of extracellular Ca^{2+} (Figure S2F), suggesting that Ca^{2+} influx was required for Ca^{2+} spikes. To determine the time course of Ca^{2+} spike development, we performed GCaMP6s imaging of C4da neurons at different time points after axotomy. Our results revealed that Ca^{2+} spike frequency gradually increased, and Ca^{2+} spikes had long-lasting duration; they began at ~12 hpa and continued at least to 30 hpa (Figure 2G). Notably, Ca^{2+} spikes described here were temporally separable from the Ca^{2+} transients associated with axotomy, the latter of which was time-locked with the laser delivery and decayed quickly (data not shown). To assess whether Ca^{2+} spikes reflect a general injury response, we severed one primary dendrite of C4da neurons using the same protocol for axotomy. Remarkably, we observed no Ca^{2+} spikes after dendritic lesion (Figure 2E), despite the fact that severed dendrites regenerate (Thompson-Peer et al., 2016). These results indicate that Ca^{2+} spikes are triggered specifically by axotomy and do not reflect general injury responses, and suggest that axon and dendrite regeneration are mechanistically different. Further supporting our conclusion that Ca^{2+} spikes are specific to axon injury, we found that exposure of larvae to UVC light, a treatment that elicits epidermal cell death and inflammatory responses around sensory neurons (Babcock et al., 2009), did not trigger Ca^{2+} spikes in C4da neurons (Figure 2E). Therefore, these Ca^{2+} spikes featured temporal and spatial characteristics; they were global Ca^{2+} signals with high amplitude, long-lasted for many hours, developed gradually over time, and were not temporally locked with axotomy.

Next, we assessed how axotomy regulates Ca^{2+} signals in C3da neurons. We detected few Ca^{2+} spikes in either intact or axotomized C3da neurons (Figure 2C-D, 2F). These results reveal that spontaneous Ca^{2+} spikes are cell type-specific, and correlate with axon regeneration competence.

The C4da neuron-specific burst firing and Ca^{2+} spikes prompted us to further investigate the relationship between these two cellular responses. To this goal, we performed extracellular recording and GCaMP6s imaging simultaneously on the same axotomized C4da neurons. We found that Ca^{2+} spikes correlated well with burst firing (Figure S2G, right panel). These results suggest that Ca^{2+} spikes derive from burst firing-induced membrane depolarization and Ca^{2+} influx, and demonstrate that Ca^{2+} spikes can serve as a surrogate for reporting burst firing. In the following studies, we will primarily use Ca^{2+} spikes to report neuronal burst firing. Supporting the notion that Ca^{2+} spikes did not report tonic firing, we did not detect Ca^{2+} spikes in intact C4da neurons (Figure S2G, left panel). Taken together, our electrophysiology and Ca^{2+} imaging experiments indicate that axotomy triggers long-lasting burst firing and resulting Ca^{2+} spikes specifically in the regenerative C4da neurons. In the current study, we referred to the long-lasting burst firing and Ca^{2+} spikes as patterned neuronal activities.

Burst Firing and Ca^{2+} spikes are Necessary for C4da Regeneration, and Sufficient to Confer C3da Regeneration

To determine if neuronal activity is necessary for axon regeneration, we expressed the inward rectifying potassium channel Kir2.1 in C4da neurons. GCaMP6s imaging confirmed that Kir2.1 overexpression reduced the Ca^{2+} spike frequency in

axotomized C4da neurons (Figure 3A-B), suggesting that burst firing is impaired. We found that Kir2.1 expression significantly reduced axon regeneration of C4da neurons (Figure 3C-D). These results suggest that burst firing and Ca^{2+} spikes are necessary for axon regeneration of C4da neurons.

We next set out to determine whether exogenously applied burst firing in C3da neurons by optogenetic stimulation can promote regeneration. We first determined the burst firing characteristics of axotomized C4da neurons by extracellular recordings (4.2 bursts per minute, 40.8 ms inter-spike interval, 7.3 action potentials per burst, Figure 1G and S3A). Next, we recorded C3da neurons expressing the light activated channelrhodopsin (ChR2) (Fenno et al., 2011) and varied the blue light stimulation intensity, duration, and frequency. We found that a 300 ms blue light pulse (470nm, 1.4 mW/mm^2) triggered a burst firing event that resembled those recorded in axotomized C4da neurons, including the inter-spike interval, the firing frequency within a burst event, and the number of AP in a burst event (Figure S3A). Because axotomized C4da neurons showed, on average, 4.2 burst firing events per minute (Figure 1F), we optogenetically delivered a 300 ms blue light pulse every 15 s to the free moving larvae bearing axotomized C3da neurons, beginning from ~6 hpa and lasting throughout the experiments (Figure 3E, lower trace and S3B-C). Remarkably, we found that optogenetically stimulated C3da neurons showed robust axon regeneration (Figure 3G-H). As an important control, we found that axon regeneration of C3da neurons was greatly diminished when any single component of the optogenetic system (Light, ChR2 or retinal) was omitted (Figure 3H).

The above experiments cannot distinguish whether the neuronal activity pattern or the overall activity increase triggers axon regeneration of C3da neurons. To distinguish between these two possibilities, we altered the optogenetic stimulation patterns, including the light pulse duration and frequency, to elicit either the tonic firing or the semi-burst firing patterns in C3da neurons (Figure 3E). Importantly, extracellular recordings showed that the burst and semi-burst firing had similar overall action potential numbers (AP/min), while the tonic firing had a slightly higher firing rate **(**Figure 3F, right panel). When examining the AP numbers per light pulse, we found semi-burst and tonic firing showed reduced AP numbers per event when compared to burst firing (6.5 AP/light pulse for burst, 2.5 for semi-burst and 1.4 for tonic; Figure 3E, left panel). If the overall activity increase underlies regeneration, optogenetically applied tonic firing will trigger stronger regeneration of C3da neurons than the burst firing does. This was not what we observed, instead we found that tonic firing triggered the least regeneration that was not statistically different from control groups, while burst firing triggered the strongest regeneration (Figure 3H). Together, these optogenetics studies indicate that exogenously applied burst firing is the most effective way to confer regeneration to C3da neurons.

If Ca^{2+} signals act downstream of neuronal excitation to promote regeneration of C3da neurons, we would expect that optogenetically applied burst, semi-burst and tonic firing induce different Ca^{2+} responses. Indeed, we found that among the three stimulation patterns, the burst firing triggered the strongest Ca^{2+} spikes (Figure 3I-L). These Ca^{2+} spikes were synchronized across the cell body, axon and dendrites, and resembled Ca^{2+} spikes detected in axotomized C4da neurons (Figure 3K). The semi-

burst firing resulted in weak Ca^{2+} spikes, and tonic firing did not produce Ca^{2+} responses (Figure 3I-J). Combining the neuronal silencing and optogenetics results, these studies suggest that Ca^{2+} spikes, which 'interpret' neuronal firing patterns, mediate axon regeneration, and suggest that the amplitude of Ca^{2+} spikes positively regulates the degree of regeneration.

L-type Ca^{2+} Channel Is Essential for Ca^{2+} Spikes and Axon Regeneration

To investigate the molecular mechanisms underlying Ca^{2+} spike generation in axotomized C4da neurons, we conducted a RNAi-based genetic screen to identify the Ca^{2+} channel responsible for Ca^{2+} spikes. We focused on Ca^{2+} channels because Ca^{2+} influx across plasma membrane was necessary for Ca^{2+} spikes (Figure S2F). *Drosophila* L-type voltage-gated calcium channel (VGCC)m is composed of the pore-forming α_1 subunits, and two auxiliary subunits β and $\alpha_2\delta$. α_1, β, and $\alpha_2\delta$ subunits are encoded by *Ca-α1D*, *Ca-beta*, and *straightjacket (stj)*, respectively (Calin-Jageman and Lee, 2008). We found that tissue-specific knockdown of either *Ca-α1D*, *Ca-beta* or *stj* decreased the Ca^{2+} spike frequency in axotomized C4da neurons (Figure S4B). Moreover, larvae bearing the Ca^{X7}/Ca^{AR66} or the Ca^{X10}/Ca^{AR66} alleles (Eberl et al., 1998), two *Ca-α1D* hypomorphic mutants, showed reduced Ca^{2+} spike frequency in axotomized C4da neurons, corroborating the RNAi results (Figure 4A-D, S4A). Nimodipine is a selective antagonist of L-type VGCCs that can block channel functions in C4da neurons (Terada et al., 2016). We found that acute application of 10 μM nimodipine significantly attenuated Ca^{2+} spike frequency in axotomized C4da neurons (Figure 4E). In contrast to the L-type VGCC (Dmca1D), we found that RNAi knockdown

of T-type VGCC (Dmca1G, or Ca-α 1T), or N-type VGCC (cacophony), had little effect on Ca^{2+} spike frequency (Figure S4C). Together, our genetic and pharmacological experiments indicate that L-type VGCC underlies axotomy-induced Ca^{2+} spikes in C4da neurons.

If Ca^{2+} spikes are required for regeneration, we would expect that manipulation of the activity of L-type VGCC has a significant impact on axon regeneration of C4da neurons. Indeed, we found that in larvae bearing *Ca-α1D* mutations or *UAS-RNAi* against *Ca-α1D* or *Ca-beta*, C4da neuron regeneration was greatly diminished (Figure 4F-G, S4D). Next, we generated the *UAS-Ca-α1D* transgenic strain, and showed that expression of *UAS-Ca-α1D* in C4da neurons completely rescued the regeneration defects of Ca^{X7}/Ca^{AR66} and Ca^{X10}/Ca^{AR66} mutants (Figure 4G). This genetic rescue study indicates that Ca-α1D acts in a cell autonomous fashion to regulate C4da neuron regeneration. Consistent with the finding that T-type VGCC did not regulate Ca^{2+} spikes (Figure S4C), we found that RNAi knockdown of Dmca1G had no effect on C4da neuron regeneration (Figure S4D), In summary, our results suggest that Ca^{2+} spikes, via the L-type VGCC activation, critically regulates axon regeneration of C4da neurons.

C4da Neurons Express Higher Levels of Ca-α1D than C3da Neurons

Because L-type VGCC regulated the Ca^{2+} spike generation in axotomized C4da neurons, we wondered if the regenerative C4da neurons have higher channel activities than the non-regenerative C3da neurons. Toward this goal, we decided to determine the *in vivo* expression levels of Ca-α1D. The lack of a specific Ca-α1D antibody prompted us to use the CRISPR-Cas9 technique to create two knock-in strains: *Ca-*

α1D-EGFP and *Ca-α1D-T2A-Gal4*, by modifying the native locus of *Ca-α1D* (Figure S4G). Here, *EGFP* and *T2A-Gal4* were inserted immediately before the stop codon. To directly measure the expression level and subcellular distribution of Ca-α1D, we performed GFP immunostaining in *Ca-α1D-EGFP* larvae. We found that the majority of Ca-α1D resided in the somatic region of sensory neurons, and immunoreactive signals in dendrites and axons were much weaker (Figure 4H-I). Nevertheless, we found Ca-α1D expression level was significantly higher in C4da than C3da neurons (Figure 4H-I). During protein translation of Ca-α1D-T2A-Gal4, Gal4 is released after T2A-mediated self-cleavage, thus can be used to map endogenous Ca-α1D expression patterns (Diao and White, 2012). By crossing *Ca-α1D-T2A-Gal4* to fluorescent reporter lines, we confirmed that Ca-α1D was expressed in larval sensory neurons, including C4da and C3da neurons (Figure 4J-K, S4H). When quantifying the nucleus fluorescent signals in larvae bearing *Ca-α1D-T2A-Gal4* and *UAS-mCherry::NLS* (NLS, nucleus localization signal), we detected stronger nucleus signals in C4da than C3da neurons (Figure 4L), consistent with the notion that C4da neurons possess a higher expression level of Ca-α1D.

Ca-α1D Overexpression Facilitates Ca^{2+} Spikes and Regeneration of C3da Neurons

Results presented so far suggest the possibility that differential expression levels of Ca-α1D might contribute to neuronal subtype-specific regeneration. To examine this idea, we expressed *UAS-Ca-α1D* specifically in C3da neurons. We found that axotomized C3da neurons overexpressing Ca-α1D did not show Ca^{2+} spikes or

increased regeneration (Figure S4E-F), suggesting that factors in addition to Ca-α1D regulate neuronal subtype-specific activities and regeneration. Because axotomy increased the overall excitability of C4da but not C3da neurons (Figure 1H, 1J), and L-type VGCC is gated by membrane depolarization, we wondered if combining Ca-α1D overexpression with neuronal activation could promote C3da neuron regeneration. Indeed, when Ca-α1D overexpression was combined with optogenetically induced tonic firing (5 ms/ 2s), a firing pattern that was ineffective by itself in promoting C3da regeneration (Figure 3H), C3da neurons exhibited significantly increased regeneration (Figure 4M-O). Next, we assessed how Ca-α1D overexpression and tonic firing, singly or combined, affected the Ca^{2+} signals in axotomized C3da neurons. We found that although Ca-α1D overexpression was ineffective in eliciting spontaneous Ca^{2+} spikes in axotomized C3da neurons (Figure S4E), tonic firing induced by optogenetics triggered robust Ca^{2+} spikes in C3da neurons overexpressing Ca-α1D (Figure 4P), suggesting that elevated Ca-α1D facilitates Ca^{2+} spike production if neuronal excitability is increased. These results suggest that L-type VGCC is not merely a permissive factor necessary for Ca^{2+} spikes and axon regeneration, instead its expression levels critically determine the amplitude of Ca^{2+} signals and subsequent regeneration strength. Together, our data are consistent with a model that patterned neuronal activities represented by Ca^{2+} spikes dictate the regeneration capacity. In C4da neurons, axotomy increased neuronal excitability and induced spontaneous burst firing, leading to strong activation of L-type VGCC and Ca^{2+} spikes; in axotomized C3da neurons, neuronal excitability was unchanged and channel activity levels were low, thus preventing Ca^{2+} spike generation. There were two ways to produce the Ca^{2+} spikes

required for C3da neuron regeneration; by optogenetically induced burst firing, or by tonic firing induction together with elevated L-type VGCC activities.

Discussion

Exogenously applied neuronal activation has been shown to promote regeneration and facilitate functional recovery (Beibei Feng et al. 2016; Li et al., 2016; Lim et al., 2016; Udina et al., 2008). However, in most cases, intrinsic activities of individual neurons have not been determined. By determining intrinsic activities at the single-cell resolution, the current study reveals that nerve injury triggers long-term modulation of neuronal excitability and Ca^{2+} signals. Remarkably, this activity modulation is cell type-specific, is triggered by axon but not dendrite injury, and mediates the cell type-specific axon regeneration. At the molecular level, we find that L-type Ca^{2+} channels are essential for Ca^{2+} spike generation and show higher expression levels in regenerative neuronal types. Collectively, our study uncovers the cellular and molecular mechanisms underlying cell type-specific regeneration, and suggests that precise control of neuronal activity patterns and Ca^{2+} dynamics represent an effective way to promote regeneration.

Nerve Injury-induced Activity Changes and Regeneration

In this study, we provide electrophysiological and Ca^{2+} imaging evidence that nerve lesion differentially modulates neuronal activities in regenerative and non-regenerative neuronal subtypes. Because C3da and C4da neurons share an almost identical local environment, it is likely this cell type-specific neuronal activity modulation

can be attributed to intrinsic differences between these two cell types. Indeed, touch-sensitive C3da and nociceptive C4da neurons differ significantly in their gene expression profiles and physiological functions (Tracey et al., 2003; Xiang et al., 2010; Yan et al., 2013). Here, we provided additional evidence to support this conclusion by showing that L-type Ca^{2+} channel displays differential expression levels between C3da and C4da neurons. It will be of interest to survey the neuronal activities and Ca^{2+} channel expression levels in other injury models and species to determine if they positively correlate with axon regeneration capacity.

One intriguing finding of the current study is that optogenetically applied burst firing is sufficient to confer regeneration to an otherwise regeneration-incompetent neuronal type. In contrast, tonic firing that elicits a similar number of action potentials fails to induce regeneration. Intracellular Ca^{2+} appears to 'interpret' neuronal activity patterns as we discovered a good correlation between burst firing, Ca^{2+} spikes and axon regeneration. These results clearly demonstrate the importance of neuronal activity patterns and Ca^{2+} dynamics in promoting of axon regeneration. Compared to neuronal activation approaches used in previous studies to promote regeneration, such as chemogenetic or visual stimulation, optogenetic stimulation offers high temporal resolution so as to precisely control neuronal activation patterns. Of note, in previous studies, neuronal activation is often less effective in promoting regeneration unless other growth promotion signaling such as mTOR is co-activated (Lim et al., 2016; Zhang et al., 2019). Hence, patterned stimulation by optogenetics represents a single component system for promoting axon regeneration. Recent developments of wireless optogenetics systems allow light to activate neurons in deep tissues (Rossi et al., 2015;

Wu et al., 2016). It will be of interest to determine if patterned stimulation by optogenetics is effective in promoting axon regeneration in other systems.

Ongoing ectopic neuronal firing in mammalian nociceptors is believed to underlie peripheral sensitization and neuropathic pain (Baron et al., 2010) . Several ion channel mechanisms have been proposed, including abnormal Na^+, K^+ channel activities (Baron et al., 2010). Given the functional and molecular conservation between larval C4da neurons and mammalian nociceptors, C4da neurons represent an excellent genetically tractable model to uncover how nerve injury alters neuronal excitability and conversely, how neuronal excitability influences the response to nerve injury.

Ca^{2+} Signaling and Axon Regeneration

Ca^{2+} transients induced by axotomy represent the earliest injury signals. In *C. elegans*, the extent of axon regeneration correlates with the amplitude of this initial Ca^{2+} transient, suggesting that Ca^{2+} levels determine the regeneration efficacy (Ghosh-Roy et al., 2010; Sun et al., 2014). Consistently, we found that optogenetically induced C3da neuron regeneration correlates with the amplitude of Ca^{2+} spikes. Despite this similarity, it is worth noting that the nature of the ongoing spontaneous Ca^{2+} spike described in this study is distinct from injury-induced Ca^{2+} transients; the former is spontaneous, takes hours to develop, has high amplitude and is synchronized across the entire C4da neurons. On the other hand, we observed a similar degree of axotomy-induced Ca^{2+} transients in C3da and C4da neurons, which decayed quickly within minutes (data not shown), suggesting that this transient Ca^{2+} increase does not regulate cell type-specific regeneration. In contrast, optogenetic stimulation starting at 6 hpa is sufficient for

promoting C3da neuron regeneration. Together, these results suggest that long-lasting spontaneous Ca^{2+} spikes, but not the acute axotomy-associated Ca^{2+} transients, promote regeneration of *Drosophila* sensory neurons.

The exact roles of Ca^{2+} signals in controlling regeneration ranges from promoting to inhibiting regeneration (Chierzi et al., 2005; Enes et al., 2010; Ghosh-Roy and Chisholm, 2010; Song et al., 2019; Tedeschi et al., 2016). Our results suggest that Ca^{2+} spikes promote C3da and C4da neuron regeneration. To reconcile our results with previous findings, we propose that the precise spatial and temporal patterns of Ca^{2+} signals, and/or the Ca^{2+} response amplitude, determine the regeneration effect. Here, axotomized C4da neurons exhibit long-lasting, high amplitude and global Ca^{2+} spikes across the entire neuron in an L-type Ca^{2+} channel-dependent manner, and the optogenetic stimulation is effective in promoting C3da neuron regeneration only when it triggers similar global Ca^{2+} spikes. As a first step to study how Ca^{2+} signals control regeneration, it will be essential to measure the detailed Ca^{2+} response dynamics in other regeneration models.

Acknowledgements

We would like to thank B. Ye for advice on optogenetic experiment setup; A. Byrne, D. Weaver, B. Ye, C. Yang, H. Liu and Y. Jan for critical comments on the manuscript; C. Wu, M. Freeman, Z. Ma, and A. Sheehan for fly lines; Bloomington Stock Center and VDRC for fly stocks; members of the Xiang lab and Song lab for helpful discussions. This work was supported by an NIH grant (5R01NS089787-01) to Y. X. and an NIH grant (1R21NS107924-01) to Y. X. and Y. S.

Author contributions

Conceptualization, K.T.P., F.W., and Y.X.; Methodology, K.T.P., F.W. Y.S., and J.G.; Investigation, K.T.P., F.W., F.L., Y.S., J.G., and P.G.; Formal Analysis, K.T.P., F.W., F.L., P.G., Y.S., and Y.X. Resources, F.W., and J.G.; Writing—Original Draft, K.T.P., F.W. and Y.X.; Writing—Review & Editing, F.L., P.G., and Y.S. Supervision, Y.X.; Funding Acquisition, Y.X.

Declaration of interests

The authors declare no conflicts of interest.

Figure 1. Subtype-specific axon regeneration correlates with neuronal activity.

(A) C4da and C3da neurons morphology. Red arrowheads indicate axons. Yellow arrowheads indicate the somata of dorsal C4da neuron (Left panel: ddaC) and dorsal C3da neurons (Middle panel: top, ddaF; bottom, ddaA). Right panel is the merge of left and middle panels. We use ddaC and ddaF as our experimental system. (B-C) Representative image of C4da neurons (B) at 24 and 48 hpa with robust regeneration and representative image of C3da neurons (C) at 24 and 48 hpa with no notable regeneration. Red circles indicate axotomy sites, red arrowheads indicate axon regrowth and yellow arrowheads indicate somata. (D-E) Quantification of regeneration including regeneration length (D) and regeneration index (E). n=25 for C4da and 12 for C3da neurons. (F) Representative electrophysiological recordings showing baseline firing of C4da and C3da intact control and axotomized neurons. Scale bar, 5s. Red box is zoomed in on outlined trace. Scale bar, 100ms. (G-H) Quantification of burst frequency of intact control and axotomized C4da (G, n=17 and 19) and C3da neurons (H, n=10 and 7). (I-J) Quantification of baseline firing frequency of intact control and axotomized C4da (I, n=17 and 19) and C3da neurons (J, n=10 and 7).

Two-tailed unpaired Student's t test (D-E, G-J). *$p<0.05$, **$p<0.01$, ***$p<0.001$, ****$p<0.0001$. n. s., not significant. Scale bar, 20 μm.

Figure 2. C4da but not C3da neuron axotomy induces spontaneous Ca^{2+} spikes. (A-D) Representative GCaMP6s calcium imaging traces of intact control (A) and axotomized (B) C4da neuron soma regions and intact control (C) and axotomized (D) C3da neuron soma regions. Left image panels are individual frames from time-lapse video at time points indicated by corresponding red arrows in right image traces. Outlined regions in (b2) indicate the regions of interest (ROIs) in soma (i), axon (ii) and dendrites (iii and iv). Right panel in (B) demonstrates that global and synchronized Ca^{2+} spikes were detected in individual ROIs (i to iv) with corresponding color. Line used in (A-B) is *w^{1118}; ; ppk-LexA, LexAop2-myr-GCaMP6s*. Line used in (C-D) is *w^{1118}; ; NompC-LexA, LexAop2-myr-GCaMP6s*. (E) Quantification of spontaneous Ca^{2+} spike frequency of C4da neurons 24 h after different treatment. n=11, 26, 10 and 10. (F) Quantification of spontaneous Ca^{2+} spike frequency of C3da neurons at 24 hpa. n=11 and 9. (G) Time course of spontaneous Ca^{2+} spike frequency after C4da neuron axotomy (set as 0 hpa). n=8, 9, 9, 9, 9, 26 and 12.

One-way ANOVA followed by Bonferroni's post hoc test (E, G) and two-tailed unpaired Student's t test (F). In (G), multiple comparisons are performed against 0 hpa group. *p<0.05, **p<0.01, ***p<0.001, ****p<0.0001. n. s., not significant. Scale bar, 20 µm.

Figure 3. Burst firing and Ca^{2+} spikes are necessary and sufficient for regeneration. (A-B) Quantification of spontaneous Ca^{2+} spike frequency of ppk-Gal4 control and Kir2.1-overexpressing C4da neurons. (A) Intact control group (n=10 and 11). (B) Axotomy group (n=10 and 10). (C) Representative image of regeneration of ppk-Gal4 control and Kir2.1-overexpressing C4da neurons. Red circles indicate axotomy sites and red arrowheads show axon regrowth. (D) Quantification of regeneration of ppk-Gal4 control and Kir2.1-overexpressing C4da neurons. n=36 and 28. (E) Representative electrophysiological recordings of C3da neurons in response to tonic, semi-burst, and burst stimulation pattern (1.4 mW/mm^2, 470nm blue light). Blue lines represent light delivery. Lines not to scale. Scale bar, 10s. Red box is zoomed in on AP firing pattern in response to first light pulse in each condition. Scale bar, 100ms. (F) Quantification of numbers of AP triggered by each light pulse (Left panel, n=11, 7 and 7) and quantification of total numbers of AP per minute in each light pattern (Right panel, n=11, 7 and 7). (G) Representative image of regeneration of C3da neurons overexpressing ChR2 with burst stimulation pattern. Red circles indicate axotomy sites and red arrowheads show axon regrowth. (H) Quantification of regeneration of C3da neurons under different conditions: 3 controls (no retinal, n=22; no ChR2, n=32; no light n=56) and 3 stimulation patterns (tonic, n=37; semi-burst, n=99; ;burst, n=115). (I-K) Representative GCaMP6s calcium imaging traces of axotomized C3da neuron (with ChR2 overexpression) soma regions at 24 hpa while delivering single tonic, semi-burst, and burst stimulation pattern (5ms, 30ms and 300ms 1.4 mW/mm^2 470nm blue light, respectively). Line used is *w^{1118}; repo-Gal80/UAS-ChR2; 19-12-Gal4/NompC-LexA, LexAop2-myr-GCaMP6s*. Right images are individual frames from time-lapse video at time points indicated by corresponding black arrows in left image traces. Red arrowheads indicate axotomized axons and yellow arrowheads indicate somata. (L) Quantification of peak GCaMP6s signal ($\Delta F/F_0$ (%)) of soma regions in axotomized C3da neurons in response to single light stimulation in (I-K). n=8, 8 and 8.

Two-tailed unpaired Student's t-test (A-B, D) and one-way ANOVA followed by Bonferroni's post hoc test (F, H and L). Bars with different superscripts in (H) are significantly different with each other ($p<0.05$). *$p<0.05$, **$p<0.01$, ***$p<0.001$, ****$p<0.0001$. n. s., not significant. Scale bar, 20 μm.

Figure 4. L-type calcium channel regulates Ca^{2+} spikes and axon regeneration.

(A-C) Representative GCaMP6s calcium imaging traces of axotomized C4da neuron soma regions. Lines used are: (A) *w^{1118}; ; ppk-LexA, LexAop2-myr-GCaMP6s*. (B) *w^{1118}; Ca-α1D^{X7}/Ca-α1D^{AR66} ; ppk-LexA, LexAop2-myr-GCaMP6s*. (C) *w^{1118}; Ca-α1D^{X7}/Ca-α1D^{AR66} ; ppk-LexA, LexAop2-myr-GCaMP6s*. Left images are individual frames from time-lapse video at time points indicated by corresponding red arrows in right image traces. Red arrowheads indicate axotomized axons. Yellow arrowheads indicate somata. (D) Quantification of spontaneous Ca^{2+} spike frequency of C4da neurons with *Ca-α1D* mutants . n=12, 9 and 9. (E) Spontaneous Ca^{2+} spikes are inhibited upon application of nimodipine (10 μM). n=13 and 13. (F) Representative image of regeneration of control, *Ca-α1D^{X7}/Ca-α1D^{AR66}* and *Ca-α1D^{X10}/Ca-α1D^{AR66}* C4da neurons. (G) Quantification of regeneration of C4da neurons with *Ca-α1D* mutants and *ppk-Gal4>Ca-α1D* rescue. n=34, 32, 41, 34 and 39. Red circles indicate axotomy sites and red arrowheads indicate axon regrowth. (H) Ca-α1D is detected in C4da and C3da neurons by immunostaining. Left three panels are from *w^{1118}* line (negative control). Right three panels are from homozygous *Ca-α1D-eGFP* line. Red HRP signal labels all neurons, while green EGFP immunostaining signal labels C4da neuron (ddaC, soma indicated by yellow arrowhead) and C3da neuron (ddaF, soma indicated by white arrowhead). Merge shows overlap. (I) Quantification of nuclear fluorescence signal in (H). n=8 and 8. (J) *ppk-EGFP* labels dorsal C4da neuron (ddaC, indicated by yellow arrowhead). *Ca-α1D-T2A-Gal4>UAS-mCherry::NLS* labels the nuclei of cells expressing Ca-α1D. Merge shows overlap. (K) *NompC-LexA>LexAop2-myr-GCaMP6s* labels two dorsal C3da neurons (top, ddaF; bottom, ddaA, indicated by white arrowheads). *Ca-α1D-T2A-Gal4>UAS-mCherry::NLS* labels the nuclei of cells expressing Ca-α1D. Merge shows overlap. (L) Quantification of nuclear mCherry::NLS fluorescence of C4da and C3da neuron soma regions from *Ca-α1D-T2A-Gal4>mCherry-NLS* larvae. n=17 and 17. (M) Representative image of regeneration of C3da neurons overexpressing ChR2 only or ChR2 with Ca-α1D with tonic stimulation pattern (5 ms/2 s, 1.4 mW/mm^2 470nm blue light) with

quantification in (O). Red circles indicate axotomy sites and red arrowheads indicate axon regrowth. (N-O) Quantification of regeneration of C3da neurons under different conditions. (N) Ca-α1D overexpression (OE) by itself in C3da neurons without light is not sufficient to promote regeneration of C3da neurons. n=58 and 58. (O) Ca-α1D OE in C3da neurons can promote regeneration when combined with tonic stimulation. n=53 and 59. (P) Ca-α1D OE in C3da neurons increases transient Ca^{2+} spike amplitude in response to single tonic stimulation pattern (5ms 26.8mW/mm^2 470nm blue light) in axotomized C3da neurons at 24 hpa. n=8 and 7. One-way ANOVA followed by Bonferroni's post hoc test (D, G), two-tailed paired student's t-test (E) and two-tailed unpaired Student's t-test (I, L, N-P). *p<0.05, **p<0.01, ***p<0.001, ****p<0.0001. n. s., not significant. Scale bar, 20 μm.

Figure S1. Related to Figure 1. Two-photon microscope-mediated specific axotomy on C4da neurons induces burst firing pattern.

(A) Schematic of axotomy of C4da neurons. VNC, ventral nerve cord. The axon of green C4da neuron is axotomized at 0 hpa. Distal axon degenerates by 24 hpa and proximal axon regenerates by 48 hpa. (B) The axon of dorsal C4da neuron is labeled with *ppk-EGFP* and glia wrapping is labeled with *Repo-Gal4>UAS-mRFP*. Left panel shows intact control and right panel shows axotomized axon with glia intact at 24 hpa. Red circle indicates axotomy site. (C-D) Definition of an event and a burst in electrophysiological recording. We define a series of consecutive AP (3 or more) with the name “event”, on condition that the inter-spike interval of each two adjacent AP is less than 100ms. (C) Average number of events per minute with indicated number of AP (‘3+’ means 3 or more, others follow the same rule) from C4da and C3da intact control and axotomized neurons. n=17, 19, 10 and 7. (D) The percentage of C4da and C3da intact control and axotomized neurons that show at least one event with indicated AP number. Events with 5 spikes or more are chosen to define a burst, since intact control C4da neurons seldom (1 of 19 cells) show events with 5 spikes or more. n=17, 19, 10 and 7. (E) Percentage of AP that is within bursts in intact control (0.171%) and axotomized (35.0%) C4da neurons. n=17 and 19. (F) Percentage of AP that is within bursts in intact control (0.0227%) and axotomized (0%) C3da neurons. n=10 and 7.

Two-tailed unpaired Student’s t test (E-F). n. s., not significant. *$p<0.05$, **$p<0.01$, ***$p<0.001$, ****$p<0.0001$. Scale bar, 5 μm.

Figure S2. Related to Figure 2. C4da neuron axotomy induces spontaneous Ca^{2+} spikes. (A) Representative GCaMP6s calcium imaging traces of axotomized C4da neuron soma region from Figure 2B after Findpeaks function by Matlab. Blue curve is normalized GCaMP6s signal. Red triangles mark the spike peak position. Red vertical lines indicate spike amplitude (prominence) based on program calculation. Orange horizontal straight lines indicate spike width. See Methods for details. (B) Quantification of spontaneous Ca^{2+} spike frequency of axotomized C4da neurons at 24 hpa based on spike amplitude distribution. n=26. (C) Accumulative percentage of spontaneous Ca^{2+} spikes of axotomized C4da neuron at 24 hpa based on spike amplitude distribution. n=146. For example, ≤25% group means the percentage of spikes with amplitude no more than 25% is 39.7%. (D-E) Spontaneous Ca^{2+} spikes of axotomized C4da neurons from Figure 2E are divided into low and high amplitude groups with an artificial cutoff of 25% amplitude. n=11, 26, 10 and 10. Only C4da axotomy group shows Ca^{2+} spikes with high amplitude. (F) Switch to 0 mM Ca^{2+} containing external solution from 1.5 mM Ca^{2+} containing solution completely blocks Ca^{2+} spikes induced by C4da neuron axotomy at 24 hpa. (G) Simultaneous calcium imaging and electrophysiological recording of intact control and axotomized C4da neurons at 24 hpa show strong temporal correlation between spontaneous Ca^{2+} spikes and burst firing. Top panel is the calcium imaging trace on soma regions. Bottom panel is simultaneous electrophysiological recording trace. Red box is zoomed in on outlined trace. Scale bar, 200ms. One-way ANOVA followed by Bonferroni's post hoc test (D-E) and two-tailed paired Student's t test (F). *$p<0.05$, **$p<0.01$, ***$p<0.001$, ****$p<0.0001$. n. s., not significant.

Figure S3. Related to Figure 3. Optogenetics light stimulation pattern setup.

(A) Blue light stimulation (300 ms 1.4 mW/mm^2 470nm) induced burst firing in C3da neurons, which shows comparable interspike interval, AP frequency within one burst, and number of AP in one burst when compared with axotomized C4da neurons at 24 hpa. (B) Schematic of ChR2 light delivery setup. (C) Schematic of optogenetics experimental procedure.

Figure S4. Related to Figure 4. L-type calcium channel regulates spontaneous Ca^{2+} spikes and axon regeneration

(A) Quantification of spontaneous Ca^{2+} spike frequency of intact control (*w^{1118}; ; ppk-LexA, LexAop2-myr-GCaMP6s*), *Ca-α1D^{X7}/Ca-α1D^{AR66}* (*w^{1118}; Ca-α1D^{X7}/Ca-α1D^{AR66} ; ppk-LexA, LexAop2-myr-GCaMP6s*) and *Ca-α1D^{X10}/Ca-α1D^{AR66}* (*w^{1118}; Ca-α1D^{X7}/Ca-α1D^{AR66} ; ppk-LexA, LexAop2-myr-GCaMP6s*). n=12, 8 and 8. (B) Quantification of spontaneous Ca^{2+} spike frequency of C4da neurons using RNAi against L-type VGCC α1 (Ca-α1D), β (Ca-beta) and $\alpha_2\delta$ (straightjacket, stj) subunits and negative control (Luciferase), n= 11, 10, 11, 12, 11 and 10. (C) Quantification of spontaneous spike frequency of C4da neurons using RNAi against Ca-α1T (T-type VGCC), cacophony (cac, N-type VGCC) and negative control (Luciferase), n=12, 13, 12 and 10. (D) Quantification of regeneration of C4da neurons using RNAi against different calcium channel subunits. n=37, 18, 38, 27, 25, 25 and 26. (E) Ca-α1D overexpression in C3da neurons does not induce spontaneous Ca^{2+} spikes after axotomy. n=10 and 10. (F) Ca-α1D overexpression in C3da neurons does not promote regeneration of C3da neurons. n=28 and 32. (G) Schematic for producing *T2A-Gal4-* or *EGFP*-tagged *Ca-α1D* line. See Methods for details. HDR, homology-directed recombination. (H) *ppk-EGFP* labels dorsal C4da neuron (ddaC, indicated by yellow arrowhead). *Ca-α1D-T2A-Gal4>UAS-mCherry* labels cells expressing Ca-α1D. White arrowheads indicate two dorsal C3da neurons (top, ddaF; bottom, ddaA). Merge shows overlap, further indicating that C4da neurons express Ca-α1D.

One-way ANOVA followed by Bonferroni's post hoc test (A-D) and two-tailed unpaired Student's t test (E-F). In (B-D), multiple comparisons are performed against the negative control group, Luciferase siRNA JF01355. *p<0.05, **p<0.01, ***p<0.001, ****p<0.0001. n. s., not significant. Scale bar, 20 µm.

Video S1-S2. GCaMP6s calcium imaging of intact control and axotomized C4da neurons at 24 hpa. Calcium signal was imaged with 0.97 Hz frame frequency. The video was played back at 10 frames per second. The left image frame is temporally synchronized with the right image trace. Region of interest is set at soma regions. Scale bar, 20 µm.

Video S1. Related to Figures 2 and S2. Intact control C4da neuron.

Video S2. Related to Figures 2 and S2. Axotomized C4da neuron.

Star methods

Key resource table

REAGENT or RESOURCE	SOURCE	IDENTIFIER
Antibodies		
Rabbit anti-GFP	Thermo Fisher	A-11122, RRID:AB_221569
HRP-conjugated Donkey anti-rabbit, HRP conjugated	GE Healthcare	NA9340, RRID:AB_772191
Alexa 488 Goat-anti-HRP	Jackson IR Lab	123-545-021, RRID:AB_2338965
Chemicals, Peptides, and Recombinant Proteins		
Paraformaldehyde	Sigma-Aldrich	P6148
Mounting media	Thermo Fisher	P36961
TES	Sigma-Aldrich	T5691
NaCl	Sigma-Aldrich	S7653
KCl	Sigma-Aldrich	P9333
$NaHCO_3$	Sigma-Aldrich	S6297
$CaCl_2$	Sigma-Aldrich	223506
$MgCl_2$	Sigma-Aldrich	M1028
Trehalose	Sigma-Aldrich	T9531
Glucose	Sigma-Aldrich	G7528
Sucrose	Sigma-Aldrich	S0389
HEPES	Sigma-Aldrich	H4034
Triton X-100	Fluka	BP151
Normal donkey serum	Sigma-Aldrich	D9663
Phosphate buffered saline (powder)	Sigma-Aldrich	P3813
Bovine serum albumin	Sigma-Aldrich	A2058
H_2O_2	Sigma-Aldrich	H1009
All-trans retinal	Sigma-Aldrich	R2500
Agarose	ThermoFisher	BP160-500
Ethanol	Decon Laboratories	Ethanol 200 proof
Isopropanol	ThermoFisher	67-63-0
Chloroform	ThermoFisher	67-66-3
Sevoflurane	Patterson Veterinary	NDC-14043-110-25
Nimodipine	Sigma-Aldrich	N149
Critical Commercial Assays		
SuperScript™ III First-Strand Synthesis System	Invitrogen	18080051
Q5 DNA polymerase	NEB	M0491S
Gibson assembly cloning kit	NEB	E5510S
TRIzol RNA Isolation Reagents	ThermoFisher	15596026
TSA Plus Cyanine 5 (Cy5) detection kit	PerkinElmer	NEL745001KT
Experimental Models: Organisms/Strains		
Drosophila, ppk-Gal4	(Xiang et al., 2010)	N/A
Drosophila, ppk-LexA	(Gou et al., 2014)	N/A
Drosophila, NompC-Gal4	Bloomington Drosophila Stock Center	#BL36369

Drosophila, ppk-CD4-tdGFP	(Han et al., 2011)	N/A
Drosophila, ppk-CD4-tdTomato	(Han et al., 2011)	N/A
Drosophila, ppk-EGFP	(Grueber et al., 2003)	N/A
Drosophila, LexAop2-myr-GCaMP6s	Laboratory of Marc Freeman	N/A
Drosophila, 19-12-Gal4	(Xiang et al., 2010)	N/A
Drosophila, Repo-Gal80	Laboratory of Marc Freeman	N/A
Drosophila, Repo-Gal4	Laboratory of Yuanquan Song	N/A
Drosophila, UAS-mRFP	Laboratory of Yuanquan Song	N/A
Drosophila, NompC-LexA	Bloomington Drosophila Stock Center	#BL52241
Drosophila, UAS-CD4-tdGFP	(Han et al., 2011)	N/A
Drosophila, UAS-2×EYFP	Bloomington Drosophila Stock Center	#BL6659
Drosophila, UAS-Kir2.1	(Baines et al., 2001; Nitabach et al., 2002)	N/A
Drosophila, UAS-ChR2::EYFP	(Hwang et al., 2007)	N/A
Drosophila, UAS-ChR2	Bloomington Drosophila Stock Center	#BL52258
Drosophila, UAS-Dicer-2	Bloomington Drosophila Stock Center	#BL24650
Drosophila, UAS-6×mCherry	Bloomington Drosophila Stock Center	#BL52268
Drosophila, UAS-mCherry::NLS	Bloomington Drosophila Stock Center	#BL38425
Drosophila, Ca^{X10}	Bloomington Drosophila Stock Center	#BL25141
Drosophila, Ca^{X7}	Bloomington Drosophila Stock Center	#BL4275
Drosophila, Ca^{AR66}	(Eberl et al., 1998)	N/A
Drosophila, UAS-Ca-α1D	This paper	N/A
Drosophila, Ca-α1D-EGFP	This paper	N/A
Drosophila, Ca-α1D-T2A-Gal4	This paper	N/A
Drosophila, hs-Cre	Bloomington Drosophila Stock Center	#BL766 #BL851
Drosophila, nos-Cas9	Bloomington Drosophila Stock Center	#BL54591
Oligonucleotides		
Ca- α1D target sequence sense: ACAATCGCCGCTAAGAGGAC	This paper	N/A
Ca- α1D target sequence anti-sense: GTCCTCTTAGCGGCGATTGT	This paper	N/A
Ca-α1D-5H'-F: GACGGTATCGATAAGCTTGATATCGACAAGTAC CAGAAACAACTTTAGCAACA	This paper	N/A
Ca-α1D-5H'-R: TGAGGAGTAAGTCTGATTGCCTTGTCCTCTTAG CGGCG	This paper	N/A
Ca-α1D-3H'-F: TATACGAAGTTATCACCCACATTGTAAGCTATAC	This paper	N/A

Ca-α1D-3H'-R: ACTAAAGGGAACAAAAGCTGGAGCTCTGTTGATCCTGATTATTGAAG	This paper	N/A
Ca-α1D-F1: ACTCTGAATAGGGAATTGGGAATTCGCCACCATGGACTTCGAGCGTGGAGC	This paper	N/A
Ca-α1D-R1: ATAGCCGATGAAAACATAATGCAACACAGG	This paper	N/A
Ca-α1D-F2: CCTGTGTTGCATTATGTTTTCATCGGCTAT	This paper	N/A
Ca-α1D-R2: GGTTCCTTCACAAAGATCCTCTAGACTATGAGGAGTAAGTCTGATTG	This paper	N/A
Recombinant DNA		
pUAST-Ca-α1D	This paper	N/A
pCFD3-Ca-α1D-gDNA	This paper	N/A
pBlueScript II SK (+) -Ca-α1D-EGFP	This paper	N/A
pBlueScript II SK (+) -Ca-α1D-T2AGal4	This paper	N/A
Software and Algorithms		
MATLAB	Mathworks	https://www.mathworks.com/
pClamp 10	Molecular Devices	https://www.moleculardevices.com/
GraphPad Prism 6	GraphPad	https://www.graphpad.com
Zen	Zeiss	N/A
ImageJ	https://imagej.nih.gov/ij/	N/A
BASIC Stamp editor v2.5	www.parallax.com	N/A
Adobe Illustrator	www.adobe.com	N/A
Adobe premiere	www.adobe.com	N/A
Other		
Drosophila low yeast brown food	Drosophila Resource Facility at UMassMed	https://www.umassmed.edu/research/cores/drosophila-resource-facility/media-recipes/
DigiTherm 38-liter Heating/Cooling Incubator (for optogenetics experiment)	Tritech research	DT2-MP-47L
Dissection scope	Zeiss	Discovery.V8
UVC crosslinker	Spectroline	Spectorlinker, 254 nm, XL-1000
Hand-held UV spectrophotometer	Spectroline	AccuMAX XS-254
Two-photon microscope	Zeiss	LSM 7 MP
Confocal fluorescence microscope	Zeiss	LSM 700
Fluorescence microscope	Zeiss	Axio Examiner.D1
Objective W Plan-Apochromat 20x/1.0 DIC M27 75mm parfocal length 75mm (FWD=1.8mm)	Zeiss	421452-9800

Objective W N-Achroplan 40x/0.75 M27 (FWD=2.1mm)	Zeiss	420967-9900
Compact light source (Mercury lamp)	Zeiss	HXP-120 V
Microelectrode puller	Sutter	P-97
Borosilicate glass capillary	World Precision Instrument	TW150-4
470nm blue LED, mounted on a 10mm square coolbase	LUXEON Rebel LED	SR-05-B0040
700mA, buckpuck DC driver	LUXEON Rebel LED	3023-D-E-700
Carclo 29.8° frosted 10mm circular beam optic-integrated legs	LUXEON Rebel LED	10413
50mm square × 25mm high alpha heat sink	LUXEON Rebel LED	N50-25B
Hand-held optical meter	Newport	1918-R
BASIC Stamp2.0 microcontroller	Parallax	N/A
Digidata 1440	Molecular Devices	https://www.moleculardevices.com
Multiclamp 700A Amplifier	Molecular Devices	https://www.moleculardevices.com

CONTACT FOR REAGENT AND RESOURCE SHARING

Further information and requests for resources and reagents should be directed to and will be fulfilled by the Lead Contact, Yang Xiang (yang.xiang@umassmed.edu).

Experiment model and subject details

Drosophila strains

All fly stocks were raised in low yeast brown food at 25°C and 60% humidity in a 12h: 12h light dark cycle unless otherwise stated. The following fly stocks are used in this study: *ppk-Gal4* (Xiang et al., 2010), *ppk-LexA* (Gou et al., 2014), *LexAop2-myr-GCaMP6s* (gift from Marc Freeman), *ppk-CD4-tdGFP* (Han et al., 2011), *ppk-CD4-tdTomato* (Han et al., 2011), *ppk-EGFP* (Grueber et al., 2003), *19-12-Gal4* (Xiang et al., 2010), *Repo-Gal80* (gift from Marc Freeman), *Repo-Gal4* (from Yuanquan Song), *UAS-mRFP* (from Yuanquan Song), *UAS-2×EYFP* (BL#6659), *NompC-Gal4* (#BL36369), *NompC-LexA* (#BL52241), *UAS-CD4-tdGFP* (Han et al., 2011), *UAS-Kir2.1* (Baines et al., 2001; Nitabach et al., 2002), *UAS-ChR2::EYFP* (Hwang et al., 2007), *UAS-ChR2* (#BL52258), *UAS-Dicer-2* (#BL24650), *UAS-6×mCherry* (#BL52268), *UAS-mCherry::NLS* (BL#38425), Ca^{X10} (#BL25141), Ca^{X7} (#BL4275) and Ca^{AR66} (gift from Chunfang Wu), *hs-Cre* (#BL766, #BL851), *nos-Cas9* (#BL54591). All RNAi lines are from Bloomington Drosophila Stock Center except siRNA KK111038 against *Ca-beta* is from Vienna Drosophila Resource Center.

Axotomy

Axotomy was performed at 80-85 h after egg laying (AEL) unless otherwise stated. We measure the axon regrowth between 24 hpa and 48 hpa time point as regeneration (Figure S1A). We followed the protocol in (Song et al., 2012) with several modifications. Briefly, a larva was anesthetized with sevofluorane vapor for 3 minutes and mounted dorsal side up. The bleaching function of a Zeiss 2-photon laser damaged a small circle (around 1.5 μm in diameter) on the axon. We found 910nm wavelength worked well for this. Axons were cut around half of the way to the bipolar dendrite, which serves as normalization marker (see Regeneration analysis part). Following axotomy, larvae were recovered on a damp Kim Wipe paper and then were transferred to recovery vials containing regular brown food (for general regeneration, calcium imaging and electrophysiology experiments) or white grape juice agar plates (for following optogenetics induction of regeneration).

Method details

Regeneration analysis

We performed quantitative analysis based on (Song et al., 2012) with some modifications. Briefly, we took two images for each neuron at 24hpa (L_1) and 48 hpa (L_2). All axon growth that occurred in this time frame was counted as regeneration. We calculated Regeneration Length as $\mathbf{L_2\text{-}L_1}$. The larvae are growing during this time period, so the Regeneration Index normalizes Regeneration Length to a fixed length in the larvae, namely, the length from the C3/4da soma to the bipolar dendrite (BD): $\mathbf{L_2/BD_2\text{-}L_1/BD_1}$.

Electrophysiology

Extracellular recording of C4da neuronal activity was performed as described previously (Xiang et al., 2010). Axotomy was performed around 80h AEL. 104□h AEL third instar larvae were dissected to make fillet preparations. Fillets were prepared in external saline solution composed

of (in mM): NaCl 120, KCl 3, $MgCl_2$ 4, $CaCl_2$ 1.5, $NaHCO_3$ 10, trehalose 10, glucose 10, TES 5, sucrose 10, HEPES 10. The Osmolality was 305 mOsm/kg and the pH was 7.25. C4da neurons (Line was *w*^{1118}*; ; ppk-EGFP*) were located under a Zeiss Axio Examiner.D1 microscope with a water immersion objective lens (Objective W N-Achroplan 40x/0.75 M27 (FWD=2.1mm)). Gentle negative pressure was applied to the C4da neuron to trap the soma in a recording pipette (5 µm tip opening; 1.5–2.0 MΩ resistance) filled with external saline solution. Recordings were performed with a 700A amplifier (Molecular Devices, Sunnyvale, CA), and the data were acquired with Digidata 1440A (Molecular Devices) and Clampex 10.6 software (Molecular Devices). Extracellular recordings of action potentials were obtained in voltage clamp mode with a holding potential of 0 mV, a 2 kHz low-pass filter and a sampling frequency of 20 kHz. The recording on C3da neurons follows the same method, except C3da neurons are labeled by *19-12-Gal4>EYFP, repo-Gal80*.

Burst analysis

For the purposes of data analysis, a burst was defined as 5 or more Aps, each having an interspike interval of less than 100ms. This definition clearly differentiated axotomized from intact control neurons (Figure S1C-E). The 'Burst Analysis' function on Clampfit 10.6 was used to detect bursts. Burst number divided by recording duration (minute) was quantified as burst frequency (bursts/min).

Calcium imaging

GCaMP6 calcium imaging of C4da neuronal activity was performed as described previously (Xiang et al., 2010). For *in vitro* calcium imaging, 3rd instar larvae at 24 hpa were pinned ventral side up on silicone elastomer plates and dissected in the same external saline solution as electrophysiology. The internal organs were removed with fine forceps and the body wall was stretched with insect pins after opening body wall. Time-lapse imaging was performed under

water objective lens (W Plan-Apochromat 20x/1.0 DIC CG=0.17 M27 75mm) by Zeiss LSM 700 confocal microscope. Frame rate is 0.97Hz. All soma ROIs were corrected for horizontal drifting with ImageJ slice alignment. Intact C4da neurons from the same 3rd instar larvae were used as negative controls.

For dendritomy in larvae, one primary dendrite branch of C4da was cut. After treatment, larvae were recovered in regular food and imaged at 24 hpa.

For UVC treated larvae, as an inflammatory nociception model (Babcock et al., 2009), larvae were mounted dorsal side up with double-sided tape on microscope slides and placed in ultraviolet crosslinker (Spectroline, XL-1000) with 20mJ/cm^2 254nm UV exposure. After treatment, larvae were recovered in regular food and imaged at 24 hpa.

Calcium imaging analysis

Each C4da or C3da neuron was imaged for 5 minutes as one sample unless otherwise stated. Original fluorescence signal (F) was firstly normalized to average intensity (F_0) of each sample by using following formula:

$$F' = (F - F_0)/F_0 * 100\%$$

After normalization, we utilized the Findpeaks function in Matlab (to find local maxima) to extract and quantify Ca^{2+} spike peaks from the noisy background. Fluorescence signals in control intact C4da neurons also show some weak and irregular Ca^{2+} spikes with small fluorescence amplitude. To rule out these weak spikes and make strong spikes stand out, we firstly calculated the standard deviation (σ) of time-lapse fluorescence signal in each control intact C4da neuron soma region at around 104h AEL larvae, then calculated the mean value of σ ($\overline{\sigma}$, n=11). We artificially set minimum peak prominence (amplitude) parameter in Findpeaks function to three fold of $\overline{\sigma}$ ($3\overline{\sigma}$, here is 14.8%) as (Figure S2A).

After acquiring position, number and amplitude (prominence) of each spike in one sample, we divided the number of spikes by recording duration (5 minutes, unless otherwise stated) as calcium spike frequency (Ca^{2+} spikes/min).

Based on these criteria, control intact C4da neurons sometimes can still show some weak spontaneous Ca^{2+} spikes. However, the amplitude of these spikes was always less than 25% (Figure S2D-E). In contrast, around 60% of spikes from axotomized C4da neurons show amplitude larger than 25% (Figure S2B-C).

For GCaMP6 calcium imaging of C3da neurons overexpressing ChR2 in Figure 3I-L, the average fluorescence signal of soma regions from 10s before the onset of light stimulation was set as F_0. The maximum fluorescence signal upon light stimulation is F_{max}. The response value $\Delta F/F_0$ (%) is quantified as:

$$\mathbf{(F_{max}-F_0)/F_0*100\%}$$

Optogenetic stimulation

The whole optogenetics setup is based on that from (Inagaki et al., 2014). Larvae were grown in regular brown food containing 400µM all-trans retinal (ATR) at 25 °C in dark condition. On 80-85 h AEL, early 3rd instar larvae were transferred from food, rinsed with water and anesthetized with sevoflurane vapor for axotomy injury. They recovered in regular brown ATR food for 6h in darkness. Next, we put them on a 35mm petri dish with 1mL white grape juice agar plates (made 1-2 days before) The grape juice agar plate formula is: 2.4g agarose, 2.6g sucrose 20mL white grape juice, 2ml 95% ethanol, then add ddH_2O to 100mL final volume. The components were microwaved to melt agarose, allowe to cool down to 65°C, then ATR was added to a final concentration, 400µM.

470nm blue LED (LUXEON Rebel LED, mounted on a 10mm square coolbase and 50mm square ×25mm high alpha heat sink, set under circular beam optic with integrated legs for parallel even light) was set over the grape juice agar plate for ChR2 activation (Figure S3B).

The light pattern was programmed with BASIC Stamp 2.0 microcontroller and buckpuck DC driver (LUXEON, 700mA, externally dimmable).

For optogenetic stimulation thereafter. At 24 and 48 hpa, axon regeneration was measured by confocal microscope (Figure S3C).

Generation of *Ca-α1D* endogenous knock-in fly lines

Alternative splicing produces 10 different CDS (coding sequence) of *Ca-α1D* annotated by Flybase (www.flybase.org). 8 of them (*Ca-α1D-PE*, *PB*, *PA*, *PC*, *PJ, PH*, *PF* and *PI*) share the same C-terminal stop codon, thus we chose to link T2A-Gal4 or EGFP tag after this C-terminus, respectively. CRISPR target sequence, 5'-ACAATCGCCGCTAAGAGGACAGG-3', is assumed to introduce a double strand DNA cut at around 20 bp upstream of this Ca-α1D stop codon. The target sequence 5'-ACAATCGCCGCTAAGAGGAC-3' (without PAM sequence AGG) was cloned to gRNA expression vector pCFD3: U6:3-gRNA (http://www.crisprflydesign.org/plasmids/). 2000 bp 5'-homology and 2000 bp 3'-homology sequence flanking the stop codon of Ca-α1D were cloned to pBlueScirpt SK(+) (Stratagene) vector after EcoRI and SacI double enzyme digestion to assist homology-directed recombination (HDR) (Figure S4G). Primer sets Ca-α1D-5H'-F and Ca-α1D-5H'-R were used to clone 5'-homology sequence. Primer sets Ca-α1D-3H'-F and Ca-α1D-3H'-R were used to clone 3'-homology sequence. gRNA expression plasmid and homology rescue plasmid were co-injected into *nos-Cas-9* (#BL54591) lines for following selection. Plasmid injection and fly transformant selection were performed by BestGene Inc. All genome-edited fly lines are confirmed by genomic DNA sequencing.

Generation of UAS-Ca-α1D transgenic fly lines

Full length cDNA of one *Drosophila Ca-α1D* isoform was cloned from total RNA extracted from w^{1118} 3rd instar larvae by RT-PCR, using TRIzol RNA isolation reagent, SuperScript III (Invitrogen), Q5 DNA polymerase (NEB lab) and Gibson Assembly Kit (NEB lab). Sequence of cDNA corresponds to the *Ca-α1D-RB* alternative isoform annotated by Flybase. For cloning of full length cDNA of *Ca-α1D*, primer sets Ca-α1D-F1 and Ca-α1D-R1 and primer sets Ca-α1D-F2 and Ca-α1D-R2 were used. cDNA was then cloned into the transgenic vector pUAST containing attB (https://www.addgene.org/vector-database/5556/) using EcoRI and XbaI double enzyme digestion. A Kozak consensus sequence (GCCACC) was introduced immediately before ATG translational start site. pUAST-Ca-α1D vectors were injected into Drosophila embryos bearing attP16 site by phiC31 integrase by BestGene Inc.. All genome-edited fly lines are confirmed by genomic DNA sequencing.

Immunostaining

We used TSA Plus Cyanine 5 (Cy5) detection kit (PerkinElmer) to boost the immunostaining signals. 3rd larvae were dissected out in ice-cold HL3 solution. HL3 solution formula is (in mM): NaCl 70, KCl 5, $MgCl_2$ 20, $NaHCO_3$ 10, trehalose 5, sucrose 115, and HEPES 5 (final pH 7.2). We used fine glass microelectrodes (pulled by P-97 microelectrode puller, Sutter) to gently remove the muscle segments covering the target C4da and C3da, since muscle cells show strong Ca-α1D expression.

Between each of the following solutions, fillets were washed with washing buffer (0.3% Triton X-100 (Sigma) in phosphate buffered saline, PBS (Sigma)) for 4 times of 15min. Larvae fillets were firstly fixed in 4% paraformaldehyde (Sigma) for 30 min at RT and then incubated in 3% H_2O_2 solution to quench endogenous peroxidase. Fillets were blocked in blocking buffer (0.3% Triton X-100, 5% donkey serum (Sigma) and 0.1% bovine serum albumin (Sigma) in PBS(Sigma)) for 1h at RT, incubated in anti-GFP primary antibody (Thermo Fisher, A-11122, 1:1500 in blocking buffer) for 40h at 4°C, and then in anti-rabbit HRP-conjugated secondary

antibody (GE Healthcare, NA9340, 1:100 in blocking buffer) for 2h at RT. Fillets were then incubated in TSA working solution (PerkinElmer, NEL745001KT) for 3min at RT and in anti-HRP antibody (Jackson immunoresearch, 123-545-021, 1:200 in blocking buffer) for 2h at RT. Fillets were finally mounted with anti-fade mountant (Thermo Fisher) for 12h at RT prior to confocal imaging.

Quantification and statistics

No statistical methods were used to pre-determine sample sizes but our sample sizes are similar to those reported in previous publications (Song et al., 2012). The values of 'n' (individual cells) are provided in the figure legends. Data are expressed as mean ± S.E.M. in bar graphs. No data points were excluded. Two-tailed unpaired or paired Student's t test was performed for comparisons between two groups of samples. One-way ANOVA followed by multiple comparison tests was performed for comparisons among three or more groups of samples. Statistical significance was assigned, *$p < 0.05$, **$p < 0.01$, ***$p < 0.001$,****$p<0.0001$.

References

Babcock, D.T., Landry, C., and Galko, M.J. (2009). Cytokine signaling mediates UV-induced nociceptive sensitization in Drosophila larvae. Current biology : CB *19*, 799-806.

Baines, R.A., Uhler, J.P., Thompson, A., Sweeney, S.T., and Bate, M. (2001). Altered electrical properties in Drosophila neurons developing without synaptic transmission. The Journal of neuroscience : the official journal of the Society for Neuroscience *21*, 1523-1531.

Baron, R., Binder, A., and Wasner, G. (2010). Neuropathic pain: diagnosis, pathophysiological mechanisms, and treatment. Lancet Neurol *9*, 807-819.

Brushart, T.M., Hoffman, P.N., Royall, R.M., Murinson, B.B., Witzel, C., and Gordon, T. (2002). Electrical stimulation promotes motoneuron regeneration without increasing its speed or conditioning the neuron. The Journal of neuroscience : the official journal of the Society for Neuroscience *22*, 6631-6638.

Calin-Jageman, I., and Lee, A. (2008). Ca(v)1 L-type Ca^{2+} channel signaling complexes in neurons. J Neurochem *105*, 573-583.

Chen, L., Wang, Z., Ghosh-Roy, A., Hubert, T., Yan, D., O'Rourke, S., Bowerman, B., Wu, Z., Jin, Y., and Chisholm, A.D. (2011). Axon regeneration pathways identified by systematic genetic screening in C. elegans. Neuron *71*, 1043-1057.

Chierzi, S., Ratto, G.M., Verma, P., and Fawcett, J.W. (2005). The ability of axons to regenerate their growth cones depends on axonal type and age, and is regulated by calcium, cAMP and ERK. Eur J Neurosci *21*, 2051-2062.

Diao, F., and White, B.H. (2012). A novel approach for directing transgene expression in Drosophila: T2A-Gal4 in-frame fusion. Genetics *190*, 1139-1144.

Duan, X., Qiao, M., Bei, F., Kim, I.J., He, Z., and Sanes, J.R. (2015). Subtype-specific regeneration of retinal ganglion cells following axotomy: effects of osteopontin and mTOR signaling. Neuron *85*, 1244-1256.

Eberl, D.F., Ren, D., Feng, G., Lorenz, L.J., Van Vactor, D., and Hall, L.M. (1998). Genetic and developmental characterization of Dmca1D, a calcium channel alpha1 subunit gene in Drosophila melanogaster. Genetics *148*, 1159-1169.

Enes, J., Langwieser, N., Ruschel, J., Carballosa-Gonzalez, M.M., Klug, A., Traut, M.H., Ylera, B., Tahirovic, S., Hofmann, F., Stein, V.*, et al.* (2010). Electrical activity suppresses axon growth through Ca(v)1.2 channels in adult primary sensory neurons. Current biology : CB *20*, 1154-1164.

Fenno, L., Yizhar, O., and Deisseroth, K. (2011). The development and application of optogenetics. Annual review of neuroscience *34*, 389-412.

Ghosh-Roy, A., and Chisholm, A.D. (2010). Caenorhabditis elegans: a new model organism for studies of axon regeneration. Dev Dyn *239*, 1460-1464.

Ghosh-Roy, A., Wu, Z., Goncharov, A., Jin, Y., and Chisholm, A.D. (2010). Calcium and cyclic AMP promote axonal regeneration in Caenorhabditis elegans and require DLK-1 kinase. The Journal of neuroscience : the official journal of the Society for Neuroscience *30*, 3175-3183.

Goldberg, J.L., Espinosa, J.S., Xu, Y., Davidson, N., Kovacs, G.T., and Barres, B.A. (2002). Retinal ganglion cells do not extend axons by default: promotion by neurotrophic signaling and electrical activity. Neuron *33*, 689-702.

Gou, B., Liu, Y., Guntur, A.R., Stern, U., and Yang, C.H. (2014). Mechanosensitive neurons on the internal reproductive tract contribute to egg-laying-induced acetic acid attraction in Drosophila. Cell reports *9*, 522-530.

Grueber, W.B., Ye, B., Moore, A.W., Jan, L.Y., and Jan, Y.N. (2003). Dendrites of distinct classes of Drosophila sensory neurons show different capacities for homotypic repulsion. Current biology : CB *13*, 618-626.

Hammarlund, M., Nix, P., Hauth, L., Jorgensen, E.M., and Bastiani, M. (2009). Axon regeneration requires a conserved MAP kinase pathway. Science (New York, NY) *323*, 802-806.

Han, C., Jan, L.Y., and Jan, Y.N. (2011). Enhancer-driven membrane markers for analysis of nonautonomous mechanisms reveal neuron-glia interactions in Drosophila. Proceedings of the National Academy of Sciences of the United States of America *108*, 9673-9678.

Hao, Y., and Collins, C. (2017). Intrinsic mechanisms for axon regeneration: insights from injured axons in Drosophila. Curr Opin Genet Dev *44*, 84-91.

He, Z., and Jin, Y. (2016). Intrinsic Control of Axon Regeneration. Neuron *90*, 437-451.

Hwang, R.Y., Zhong, L., Xu, Y., Johnson, T., Zhang, F., Deisseroth, K., and Tracey, W.D. (2007). Nociceptive neurons protect Drosophila larvae from parasitoid wasps. Current biology : CB *17*, 2105-2116.

Inagaki, H.K., Jung, Y., Hoopfer, E.D., Wong, A.M., Mishra, N., Lin, J.Y., Tsien, R.Y., and Anderson, D.J. (2014). Optogenetic control of Drosophila using a red-shifted channelrhodopsin reveals experience-dependent influences on courtship. Nat Methods *11*, 325-332.

Kamber, D., Erez, H., and Spira, M.E. (2009). Local calcium-dependent mechanisms determine whether a cut axonal end assembles a retarded endbulb or competent growth cone. Exp Neurol *219*, 112-125.

Li, S., Yang, C., Zhang, L., Gao, X., Wang, X., Liu, W., Wang, Y., Jiang, S., Wong, Y.H., Zhang, Y.*, et al.* (2016). Promoting axon regeneration in the adult CNS by modulation of the melanopsin/GPCR signaling. Proceedings of the National Academy of Sciences of the United States of America *113*, 1937-1942.

Lim, J.H., Stafford, B.K., Nguyen, P.L., Lien, B.V., Wang, C., Zukor, K., He, Z., and Huberman, A.D. (2016). Neural activity promotes long-distance, target-specific regeneration of adult retinal axons. Nature neuroscience *19*, 1073-1084.

Nitabach, M.N., Blau, J., and Holmes, T.C. (2002). Electrical silencing of Drosophila pacemaker neurons stops the free-running circadian clock. Cell *109*, 485-495.

Park, K.K., Liu, K., Hu, Y., Smith, P.D., Wang, C., Cai, B., Xu, B., Connolly, L., Kramvis, I., Sahin, M.*, et al.* (2008). Promoting axon regeneration in the adult CNS by modulation of the PTEN/mTOR pathway. Science (New York, NY) *322*, 963-966.

Rossi, M.A., Go, V., Murphy, T., Fu, Q., Morizio, J., and Yin, H.H. (2015). A wirelessly controlled implantable LED system for deep brain optogenetic stimulation. Front Integr Neurosci *9*, 8.

Shin, J.E., Cho, Y., Beirowski, B., Milbrandt, J., Cavalli, V., and DiAntonio, A. (2012). Dual leucine zipper kinase is required for retrograde injury signaling and axonal regeneration. Neuron *74*, 1015-1022.

Singh, K.K., and Miller, F.D. (2005). Activity regulates positive and negative neurotrophin-derived signals to determine axon competition. Neuron *45*, 837-845.

Song, Y., Li, D., Farrelly, O., Miles, L., Li, F., Kim, S.E., Lo, T.Y., Wang, F., Li, T., Thompson-Peer, K.L.*, et al.* (2019). The Mechanosensitive Ion Channel Piezo Inhibits Axon Regeneration. Neuron *102*, 373-389 e376.

Song, Y., Ori-McKenney, K.M., Zheng, Y., Han, C., Jan, L.Y., and Jan, Y.N. (2012). Regeneration of Drosophila sensory neuron axons and dendrites is regulated by the Akt pathway involving Pten and microRNA bantam. Genes Dev *26*, 1612-1625.

Spitzer, N.C. (2006). Electrical activity in early neuronal development. Nature *444*, 707-712.

Sun, L., Shay, J., McLoed, M., Roodhouse, K., Chung, S.H., Clark, C.M., Pirri, J.K., Alkema, M.J., and Gabel, C.V. (2014). Neuronal regeneration in C. elegans requires subcellular calcium release by ryanodine receptor channels and can be enhanced by optogenetic stimulation. The Journal of neuroscience : the official journal of the Society for Neuroscience *34*, 15947-15956.

Tedeschi, A., and Bradke, F. (2013). The DLK signalling pathway--a double-edged sword in neural development and regeneration. EMBO Rep *14*, 605-614.

Tedeschi, A., Dupraz, S., Laskowski, C.J., Xue, J., Ulas, T., Beyer, M., Schultze, J.L., and Bradke, F. (2016). The Calcium Channel Subunit Alpha2delta2 Suppresses Axon Regeneration in the Adult CNS. Neuron *92*, 419-434.

Terada, S., Matsubara, D., Onodera, K., Matsuzaki, M., Uemura, T., and Usui, T. (2016). Neuronal processing of noxious thermal stimuli mediated by dendritic Ca(2+) influx in Drosophila somatosensory neurons. eLife *5*.

Thompson-Peer, K.L., DeVault, L., Li, T., Jan, L.Y., and Jan, Y.N. (2016). In vivo dendrite regeneration after injury is different from dendrite development. Genes Dev *30*, 1776-1789.

Tracey, W.D., Jr., Wilson, R.I., Laurent, G., and Benzer, S. (2003). painless, a Drosophila gene essential for nociception. Cell *113*, 261-273.

Wu, X., Zhang, Y., Takle, K., Bilsel, O., Li, Z., Lee, H., Zhang, Z., Li, D., Fan, W., Duan, C., *et al.* (2016). Dye-Sensitized Core/Active Shell Upconversion Nanoparticles for Optogenetics and Bioimaging Applications. ACS Nano *10*, 1060-1066.

Xiang, Y., Yuan, Q., Vogt, N., Looger, L.L., Jan, L.Y., and Jan, Y.N. (2010). Light-avoidance-mediating photoreceptors tile the Drosophila larval body wall. Nature *468*, 921-926.

Xiong, X., Wang, X., Ewanek, R., Bhat, P., Diantonio, A., and Collins, C.A. (2010). Protein turnover of the Wallenda/DLK kinase regulates a retrograde response to axonal injury. J Cell Biol *191*, 211-223.

Yan, D., Wu, Z., Chisholm, A.D., and Jin, Y. (2009). The DLK-1 kinase promotes mRNA stability and local translation in C. elegans synapses and axon regeneration. Cell *138*, 1005-1018.

Yan, Z., Zhang, W., He, Y., Gorczyca, D., Xiang, Y., Cheng, L.E., Meltzer, S., Jan, L.Y., and Jan, Y.N. (2013). Drosophila NOMPC is a mechanotransduction channel subunit for gentle-touch sensation. Nature *493*, 221-225.

Zhang, L.I., and Poo, M.M. (2001). Electrical activity and development of neural circuits. Nature neuroscience *4 Suppl*, 1207-1214.

Zhang, Y., Williams, P.R., Jacobi, A., Wang, C., Goel, A., Hirano, A.A., Brecha, N.C., Kerschensteiner, D., and He, Z. (2019). Elevating Growth Factor Responsiveness and Axon Regeneration by Modulating Presynaptic Inputs. Neuron *103*, 39-51 e35.

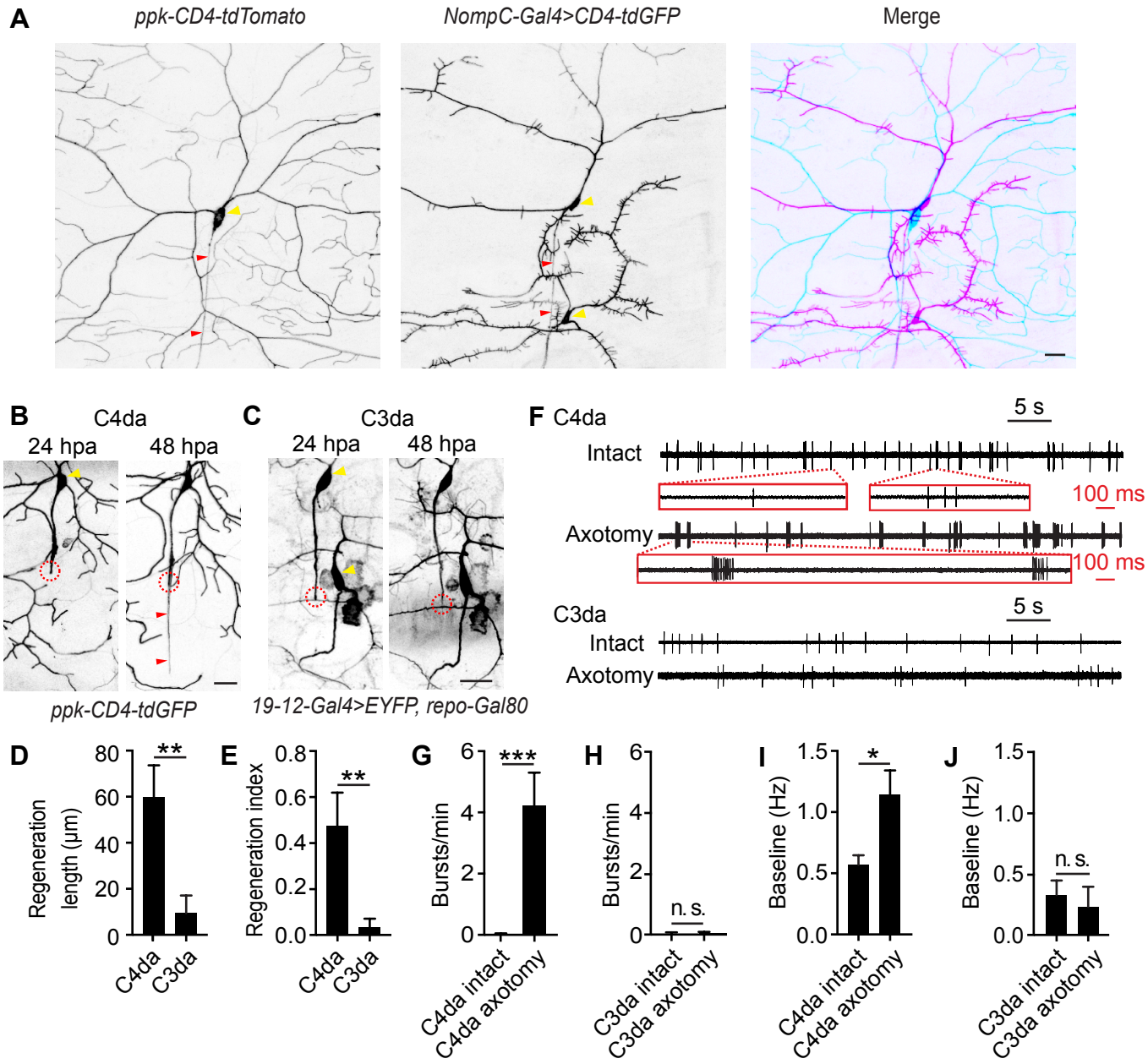
A
ppk-CD4-tdTomato
NompC-Gal4>CD4-tdGFP
Merge
B
C4da
24 hpa
48 hpa
C
C3da
24 hpa
48 hpa
ppk-CD4-tdGFP
19-12-Gal4>EYFP, repo-Gal80
F
C4da
5 s
Intact
100 ms
Axotomy
100 ms
C3da
5 s
Intact
Axotomy
D
Regeneration length (μm)
80
60
40
20
0
**
C4da
C3da
E
Regeneration index
0.8
0.6
0.4
0.2
0.0
**
C4da
C3da
G
Bursts/min
6
4
2
0
***
C4da intact
C4da axotomy
H
Bursts/min
6
4
2
0
n. s.
C3da intact
C3da axotomy
I
Baseline (Hz)
1.5
1.0
0.5
0.0
*
C4da intact
C4da axotomy
J
Baseline (Hz)
1.5
1.0
0.5
0.0
n. s.
C3da intact
C3da axotomy

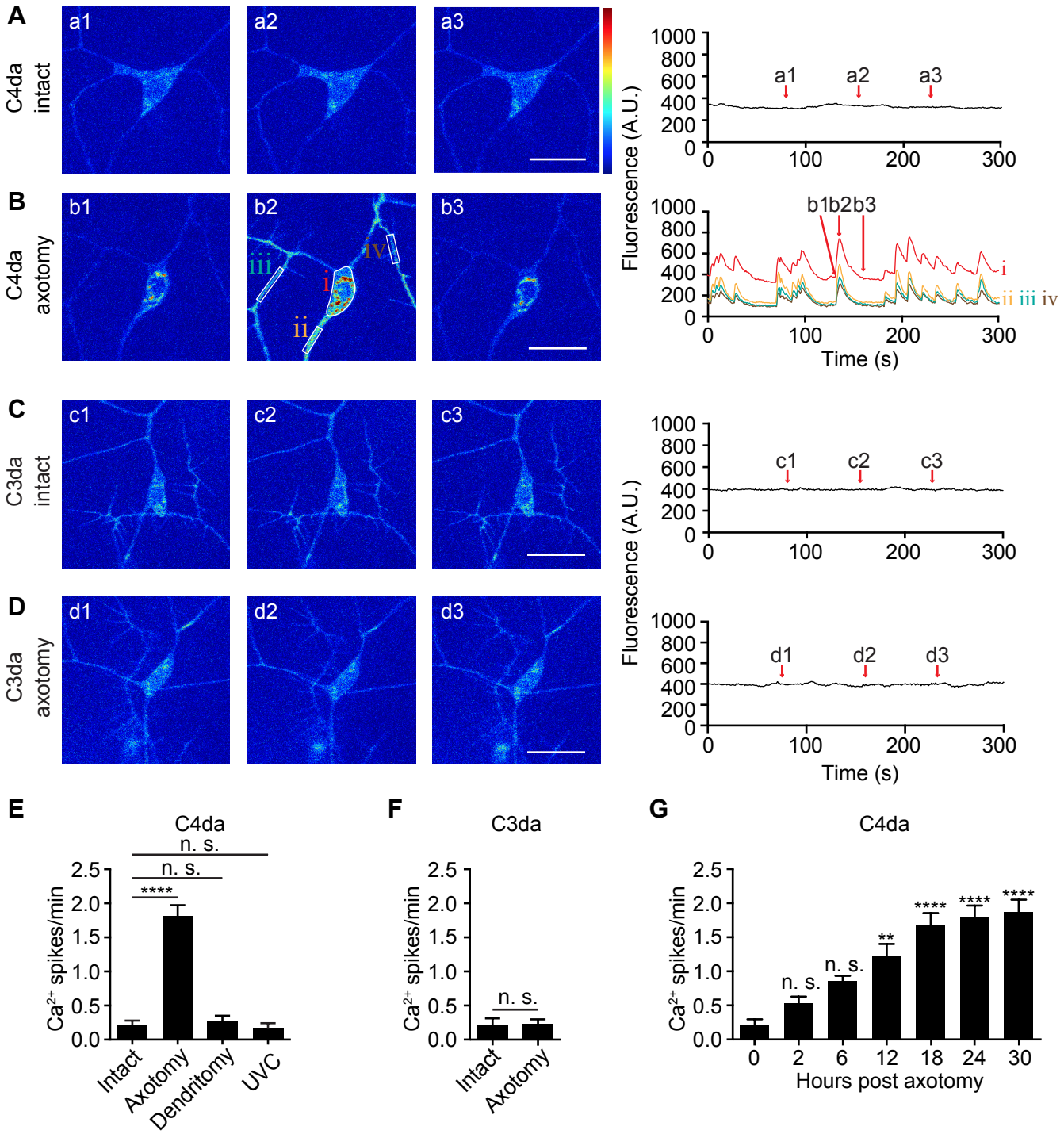
A
C4da
intact
a1
a2
a3
B
C4da
axotomy
b1
b2
b3
i
ii
iii
iv
C
C3da
intact
c1
c2
c3
D
C3da
axotomy
d1
d2
d3
Fluorescence (A.U.)
Time (s)
b1b2b3
E
C4da
Ca2+ spikes/min
n. s.
****
Intact
Axotomy
Dendritomy
UVC
F
C3da
n. s.
Intact
Axotomy
G
C4da
n. s.
**
****
Hours post axotomy

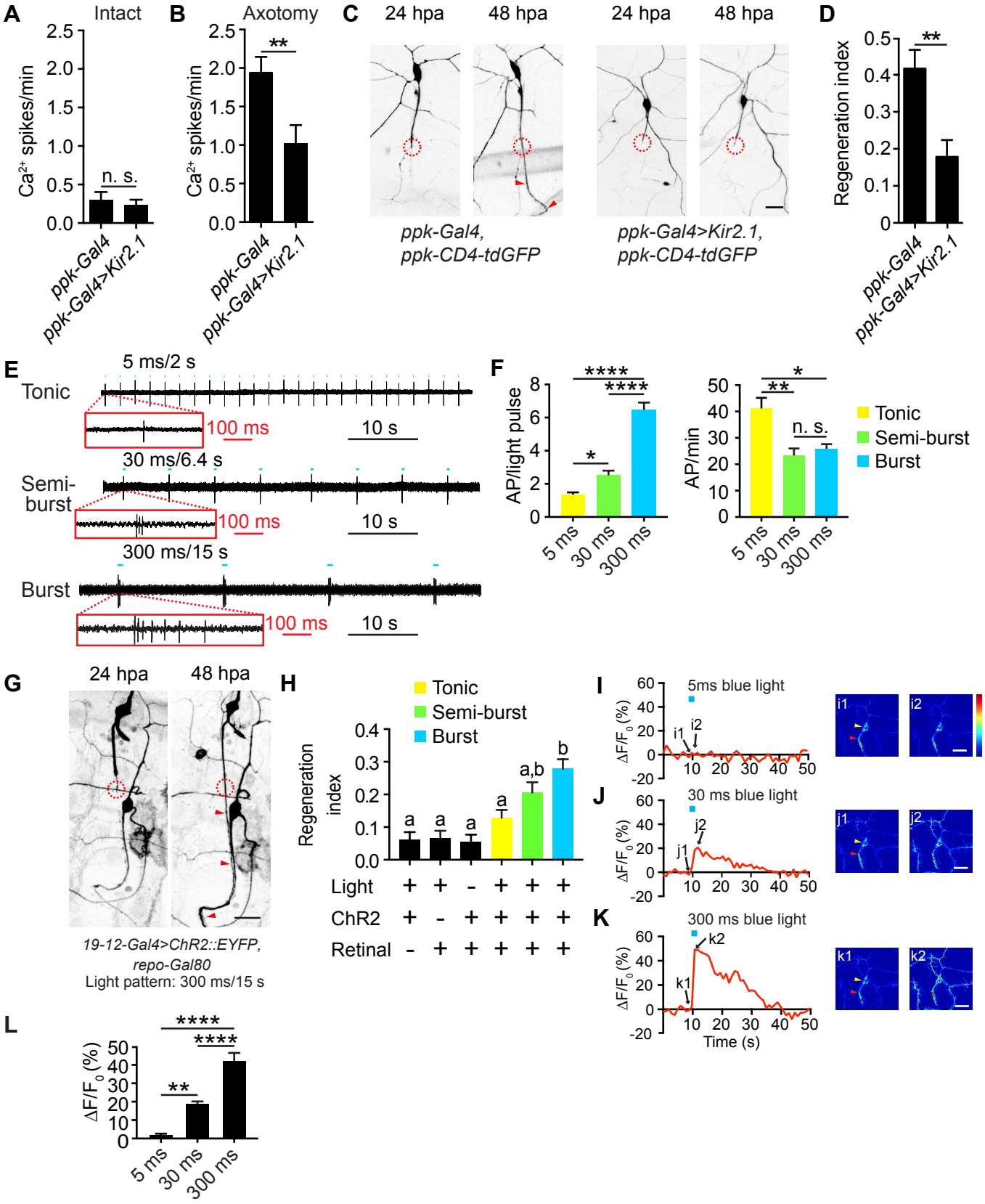
A
Intact
Ca2+ spikes/min
2.5
2.0
1.5
1.0
0.5
0.0
n. s.
ppk-Gal4
ppk-Gal4>Kir2.1
B
Axotomy
Ca2+ spikes/min
**
ppk-Gal4
ppk-Gal4>Kir2.1
C
24 hpa
48 hpa
24 hpa
48 hpa
ppk-Gal4,
ppk-CD4-tdGFP
ppk-Gal4>Kir2.1,
ppk-CD4-tdGFP
D
Regeneration index
0.5
0.4
0.3
0.2
0.1
0
**
ppk-Gal4
ppk-Gal4>Kir2.1
E
5 ms/2 s
Tonic
100 ms
10 s
30 ms/6.4 s
Semi-burst
100 ms
10 s
300 ms/15 s
Burst
100 ms
10 s
F
AP/light pulse
8
6
4
2
0
****
****
*
5 ms
30 ms
300 ms
AP/min
50
40
30
20
10
0
*
**
n. s.
5 ms
30 ms
300 ms
Tonic
Semi-burst
Burst
G
24 hpa
48 hpa
19-12-Gal4>ChR2::EYFP,
repo-Gal80
Light pattern: 300 ms/15 s
H
Tonic
Semi-burst
Burst
Regeneration index
0.4
0.3
0.2
0.1
0.0
a
a
a
a
a,b
b
Light + + - + + +
ChR2 + - + + + +
Retinal - + + + + +
I
5ms blue light
ΔF/F0 (%)
60
40
20
0
-20
i1
i2
10 20 30 40 50
J
30 ms blue light
j1
j2
K
300 ms blue light
k1
k2
Time (s)
L
ΔF/F0 (%)
50
40
30
20
10
0
**
****
****
5 ms
30 ms
300 ms

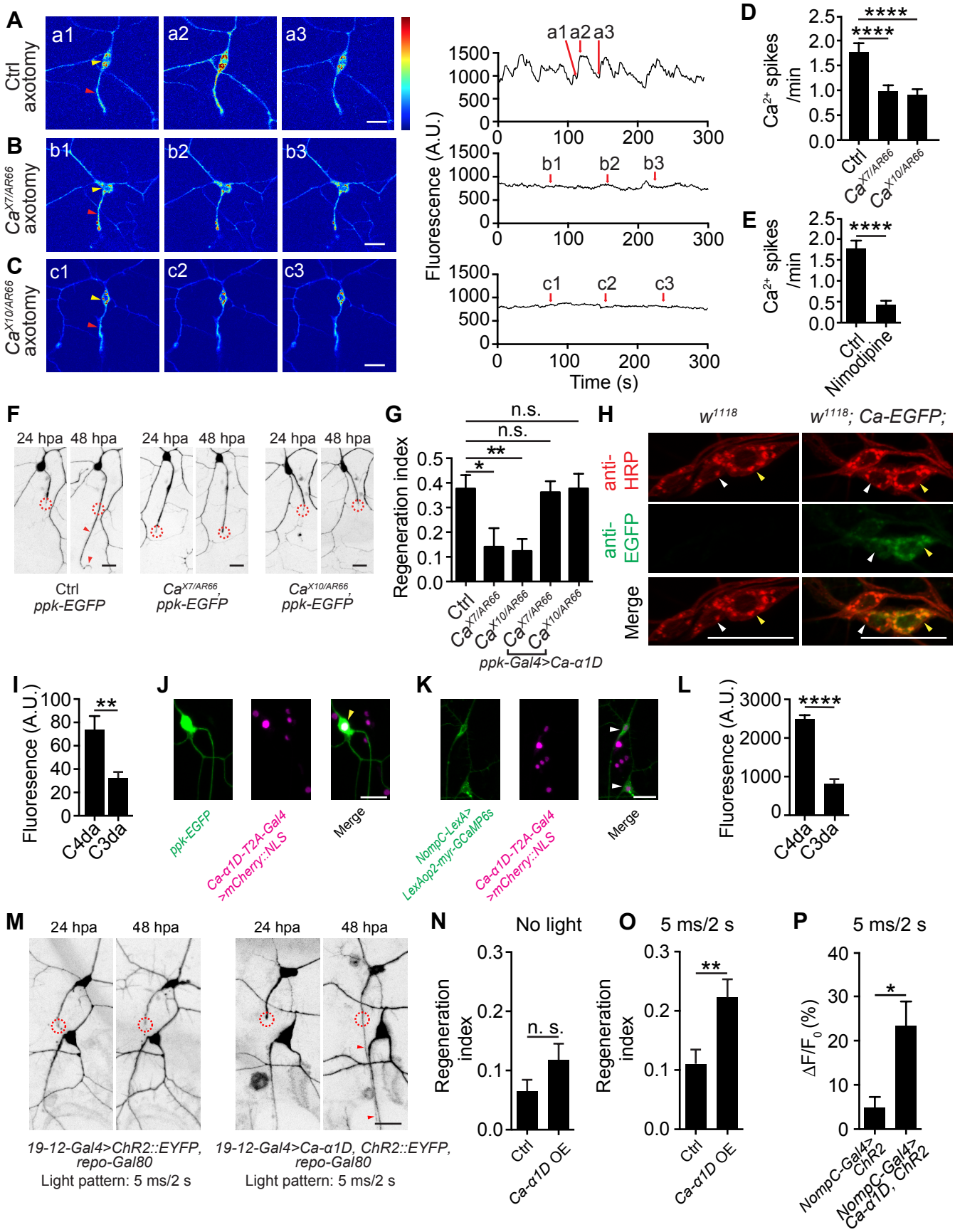
A
Ctrl axotomy
a1
a2
a3
B
Ca^X7/AR66 axotomy
b1
b2
b3
C
Ca^X10/AR66 axotomy
c1
c2
c3
Fluorescence (A.U.)
Time (s)
D
Ca2+ spikes /min
Ctrl
Ca^X7/AR66
Ca^X10/AR66
E
Ca2+ spikes /min
Ctrl
Nimodipine
F
24 hpa
48 hpa
Ctrl ppk-EGFP
Ca^X7/AR66, ppk-EGFP
Ca^X10/AR66, ppk-EGFP
G
Regeneration index
n.s.
n.s.
ppk-Gal4>Ca-α1D
H
w1118
w1118; Ca-EGFP;
anti-HRP
anti-EGFP
Merge
I
Fluoresence (A.U.)
C4da
C3da
J
ppk-EGFP
Ca-α1D-T2A-Gal4 >mCherry::NLS
Merge
K
NompC-LexA> LexAop2-myr-GCaMP6s
Ca-α1D-T2A-Gal4 >mCherry::NLS
Merge
L
Fluoresence (A.U.)
C4da
C3da
M
24 hpa
48 hpa
19-12-Gal4>ChR2::EYFP, repo-Gal80
Light pattern: 5 ms/2 s
19-12-Gal4>Ca-α1D, ChR2::EYFP, repo-Gal80
Light pattern: 5 ms/2 s
N
No light
Regeneration index
n. s.
Ctrl
Ca-α1D OE
O
5 ms/2 s
Regeneration index
Ctrl
Ca-α1D OE
P
5 ms/2 s
ΔF/F0 (%)
NompC-Gal4> ChR2
NompC-Gal4> Ca-α1D, ChR2

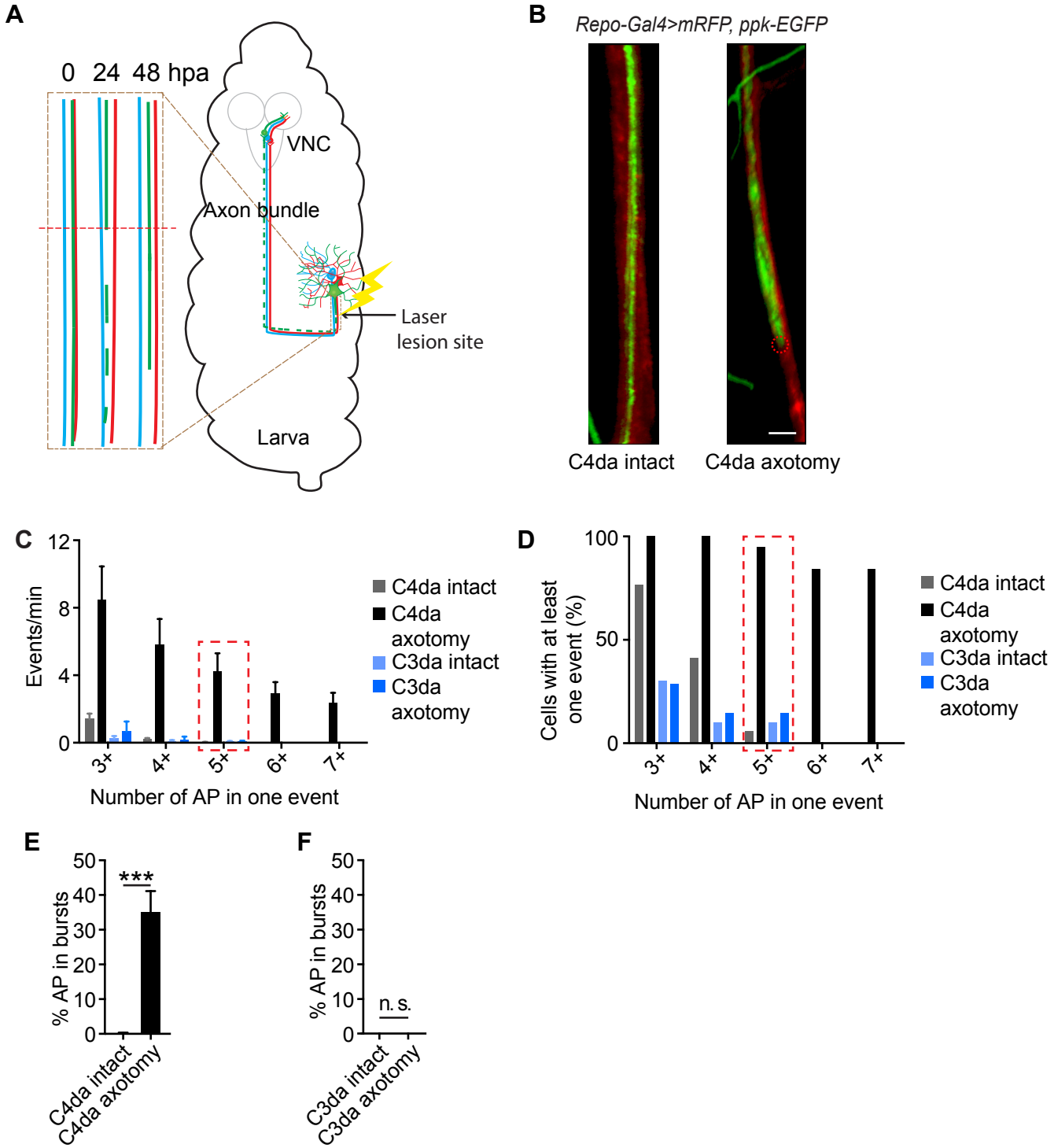
A
0 24 48 hpa
VNC
Axon bundle
Laser
lesion site
Larva
B
Repo-Gal4>mRFP, ppk-EGFP
C4da intact
C4da axotomy
C
Events/min
12
8
4
0
3+
4+
5+
6+
7+
Number of AP in one event
C4da intact
C4da axotomy
C3da intact
C3da axotomy
D
Cells with at least one event (%)
100
50
0
3+
4+
5+
6+
7+
Number of AP in one event
C4da intact
C4da axotomy
C3da intact
C3da axotomy
E
% AP in bursts
50
40
30
20
10
0
***
C4da intact
C4da axotomy
F
% AP in bursts
50
40
30
20
10
0
n. s.
C3da intact
C3da axotomy

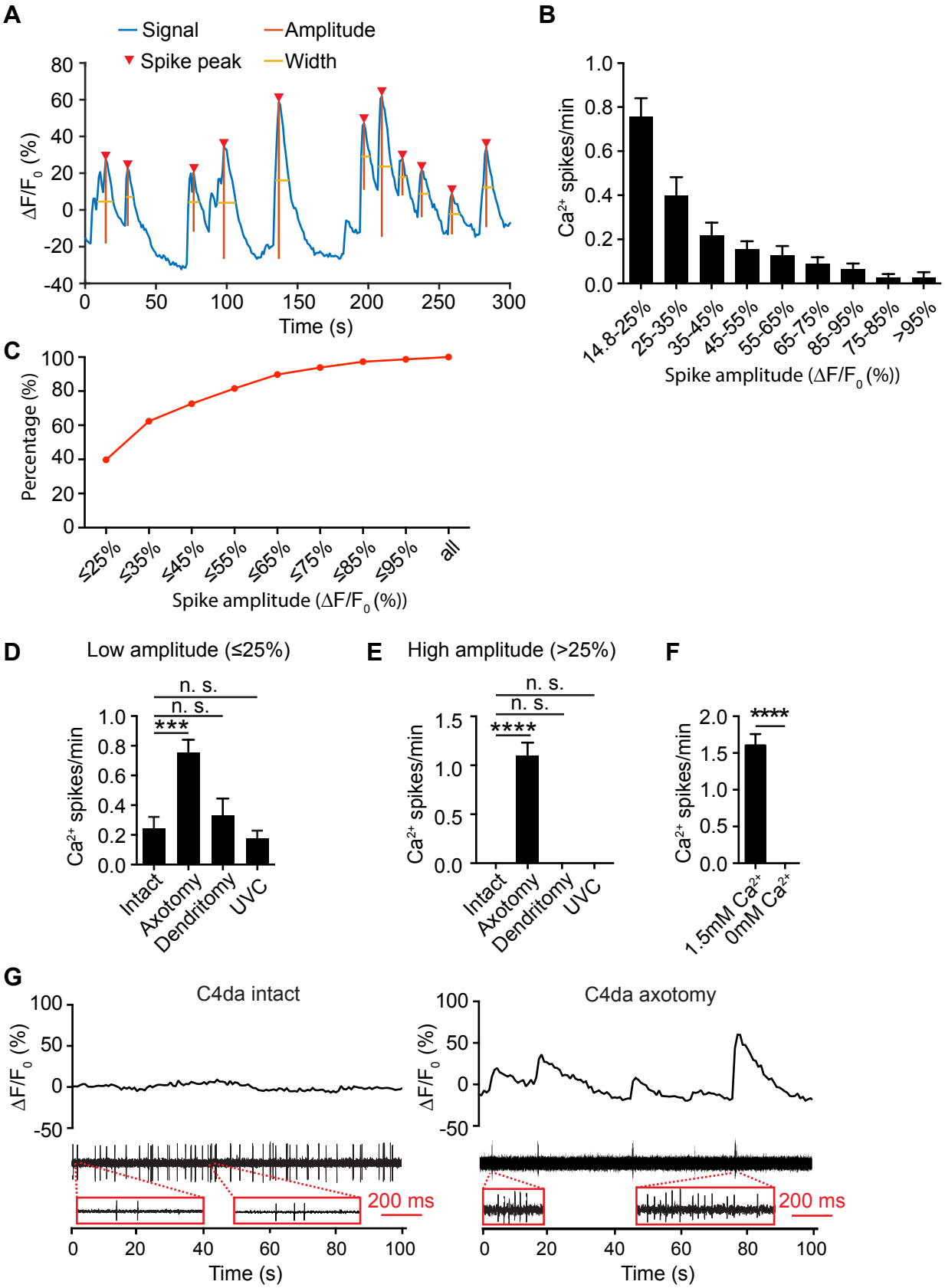
A
Signal
Amplitude
Spike peak
Width
ΔF/F0 (%)
Time (s)
B
Ca2+ spikes/min
14.8-25%
25-35%
35-45%
45-55%
55-65%
65-75%
85-95%
75-85%
>95%
Spike amplitude (ΔF/F0 (%))
C
Percentage (%)
≤25%
≤35%
≤45%
≤55%
≤65%
≤75%
≤85%
≤95%
all
Spike amplitude (ΔF/F0 (%))
D
Low amplitude (≤25%)
n. s.
n. s.
***
Ca2+ spikes/min
Intact
Axotomy
Dendritomy
UVC
E
High amplitude (>25%)
n. s.
n. s.
****
Ca2+ spikes/min
Intact
Axotomy
Dendritomy
UVC
F
****
Ca2+ spikes/min
1.5mM Ca2+
0mM Ca2+
G
C4da intact
C4da axotomy
ΔF/F0 (%)
200 ms
Time (s)

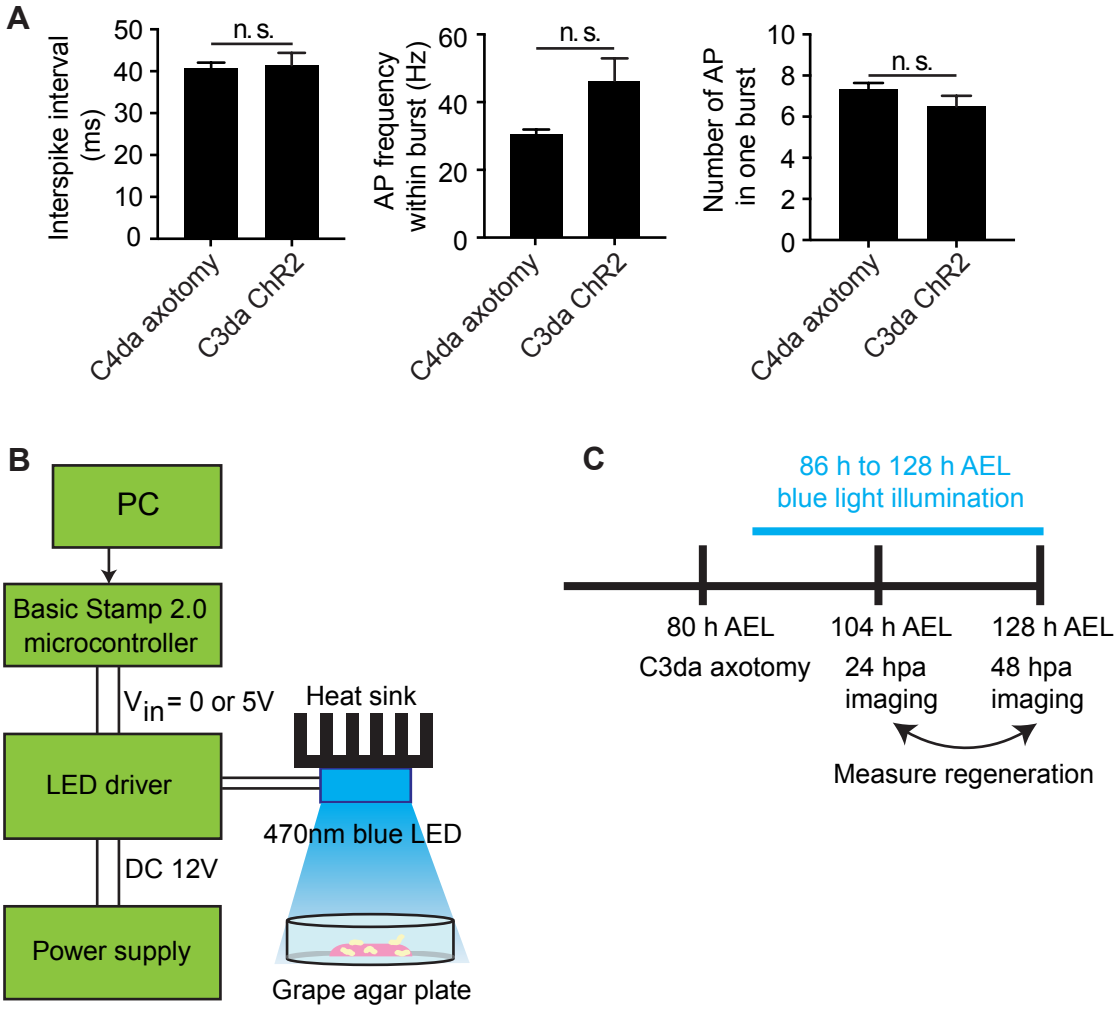
A
Interspike interval (ms)
50
40
30
20
10
0
n. s.
C4da axotomy
C3da ChR2
AP frequency within burst (Hz)
60
40
20
0
n. s.
C4da axotomy
C3da ChR2
Number of AP in one burst
10
8
6
4
2
0
n. s.
C4da axotomy
C3da ChR2
B
PC
Basic Stamp 2.0 microcontroller
V_{in} = 0 or 5V
Heat sink
LED driver
470nm blue LED
DC 12V
Power supply
Grape agar plate
C
86 h to 128 h AEL
blue light illumination
80 h AEL
C3da axotomy
104 h AEL
24 hpa imaging
128 h AEL
48 hpa imaging
Measure regeneration

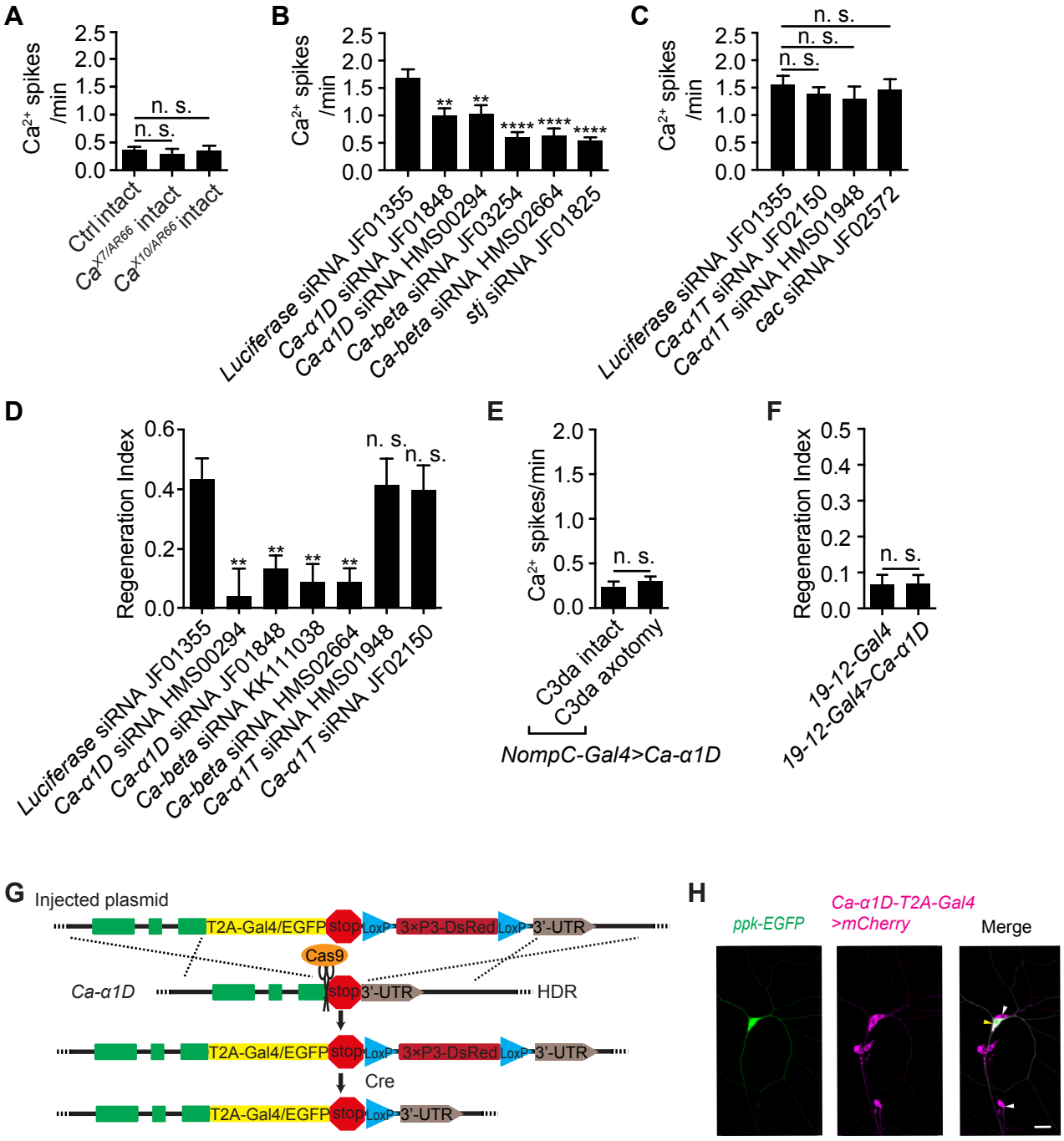
A
Ca2+ spikes /min
2.5
2.0
1.5
1.0
0.5
0.0
n. s.
n. s.
Ctrl intact
CaX7/AR66 intact
CaX10/AR66 intact
B
Ca2+ spikes /min
**
**
****
****
****
Luciferase siRNA JF01355
Ca-α1D siRNA JF01848
Ca-α1D siRNA HMS00294
Ca-beta siRNA JF03254
Ca-beta siRNA HMS02664
stj siRNA JF01825
C
Ca2+ spikes /min
n. s.
n. s.
n. s.
Luciferase siRNA JF01355
Ca-α1T siRNA JF02150
Ca-α1T siRNA HMS01948
cac siRNA JF02572
D
Regeneration Index
0.6
0.4
0.2
0.0
**
**
**
**
n. s.
n. s.
Luciferase siRNA JF01355
Ca-α1D siRNA HMS00294
Ca-α1D siRNA JF01848
Ca-beta siRNA KK111038
Ca-beta siRNA HMS02664
Ca-α1T siRNA HMS01948
Ca-α1T siRNA JF02150
E
Ca2+ spikes/min
2.0
1.5
1.0
0.5
0.0
n. s.
C3da intact
C3da axotomy
NompC-Gal4>Ca-α1D
F
Regeneration Index
0.5
0.4
0.3
0.2
0.1
0.0
n. s.
19-12-Gal4
19-12-Gal4>Ca-α1D
G
Injected plasmid
T2A-Gal4/EGFP
stop
LoxP
3×P3-DsRed
LoxP
3'-UTR
Cas9
Ca-α1D
stop
3'-UTR
HDR
T2A-Gal4/EGFP
stop
LoxP
3×P3-DsRed
LoxP
3'-UTR
Cre
T2A-Gal4/EGFP
stop
LoxP
3'-UTR
H
ppk-EGFP
Ca-α1D-T2A-Gal4 >mCherry
Merge